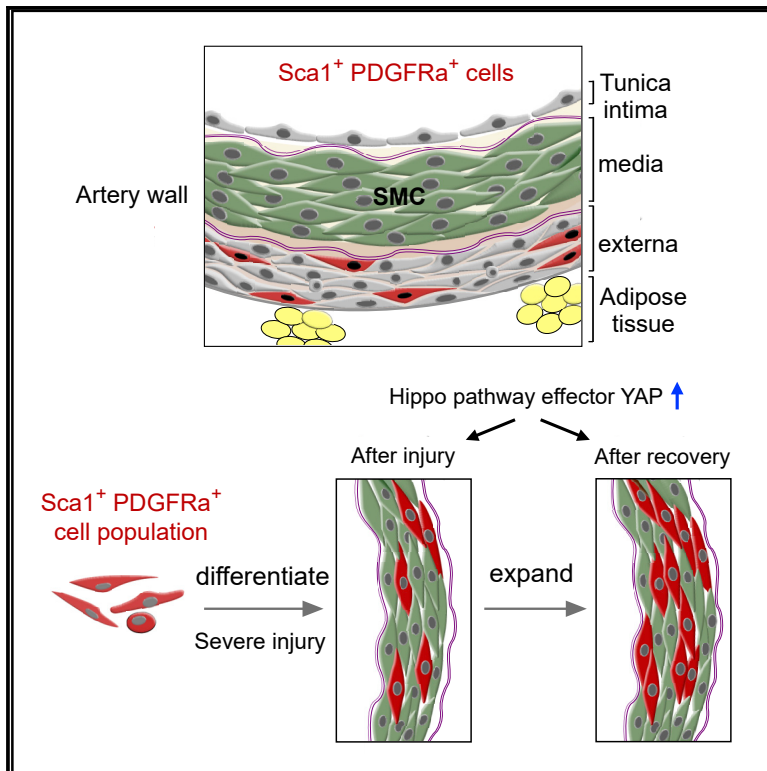


Arterial Sca1⁺ Vascular Stem Cells Generate *De Novo* Smooth Muscle for Artery Repair and Regeneration

Graphical Abstract



Authors

Juan Tang, Haixiao Wang, Xiuzhen Huang, ..., Li Zhang, Dong Gao, Bin Zhou

Correspondence

li_zhang@zju.edu.cn (L.Z.),
dong.gao@sibcb.ac.cn (D.G.),
zhoubin@sibs.ac.cn (B.Z.)

In Brief

Tang et al. show that Sca1⁺PDGFRa⁺ cells in the adventitial layer of arteries are resident vascular stem cells that produce new smooth muscle cells (SMCs) in response to injury. Sca1-derived SMCs expand more efficiently than pre-existing SMCs during vessel repair, which is regulated by the Hippo pathway effector YAP.

Highlights

- Sca1⁺ vascular stem cells produce new smooth muscle cells after severe vessel injury
- A Sca1⁺PDGFRa⁺ subpopulation contributes to vascular repair and regeneration
- Sca1-derived smooth muscle cells expand more than pre-existing smooth muscle
- YAP is required for Sca1-derived smooth muscle cell expansion during vascular repair



Arterial Sca1⁺ Vascular Stem Cells Generate *De Novo* Smooth Muscle for Artery Repair and Regeneration

Juan Tang,^{1,12} Haixiao Wang,^{1,12} Xiuzhen Huang,^{1,12} Fei Li,^{1,12} Huan Zhu,¹ Yan Li,¹ Lingjuan He,¹ Hui Zhang,² Wenjuan Pu,¹ Kuo Liu,^{1,2} Huan Zhao,¹ Jacob Fog Bentzon,^{3,4} Ying Yu,⁵ Yong Ji,^{6,7} Yu Nie,⁸ Xueying Tian,⁹ Li Zhang,^{10,*} Dong Gao,^{1,11,*} and Bin Zhou^{1,2,9,11,13,*}

¹The State Key Laboratory of Cell Biology, CAS Center for Excellence in Molecular Cell Science, Shanghai Institute of Biochemistry and Cell Biology, University of Chinese Academy of Sciences, Chinese Academy of Sciences, Shanghai 200031, China

²School of Life Science and Technology, ShanghaiTech University, Shanghai 201210, China

³Centro Nacional de Investigaciones Cardiovasculares Carlos III, Madrid, Spain

⁴Department of Clinical Medicine, Aarhus University, Aarhus, Denmark

⁵Department of Pharmacology and Tianjin Key Laboratory of Inflammatory Biology, Key Laboratory of Immune Microenvironment and Disease (Ministry of Education), School of Basic Medical Sciences, Tianjin Medical University, Tianjin 300070, China

⁶Key Laboratory of Cardiovascular and Cerebrovascular Medicine, Nanjing Medical University, Nanjing 211100, China

⁷The Collaborative Innovation Center for Cardiovascular Disease Translational Medicine, Nanjing Medical University, Nanjing 211100, China

⁸State Key Laboratory of Cardiovascular Disease, Fuwai Hospital, National Center for Cardiovascular Disease, Chinese Academy of Medical Sciences and Peking Union Medical College, Beijing, China

⁹Key Laboratory of Regenerative Medicine of the Ministry of Education, Jinan University, Guangzhou 510632, China

¹⁰The Department of Cardiology, First Affiliated Hospital, School of Medicine, Zhejiang University, Hangzhou, China

¹¹Institute for Stem Cell and Regeneration, Chinese Academy of Sciences, Beijing, China

¹²These authors contributed equally

¹³Lead Contact

*Correspondence: li_zhang@zju.edu.cn (L.Z.), dong.gao@sibcb.ac.cn (D.G.), zhoubin@sibs.ac.cn (B.Z.)

<https://doi.org/10.1016/j.stem.2019.11.010>

SUMMARY

Rapid regeneration of smooth muscle after vascular injury is essential for maintaining arterial function. The existence and putative roles of resident vascular stem cells (VSCs) in artery repair are controversial, and vessel regeneration is thought to be mediated by proliferative expansion of pre-existing smooth muscle cells (SMCs). Here, we performed cell fate mapping and single-cell RNA sequencing to identify Sca1⁺ VSCs in the adventitial layer of artery walls. After severe injury, Sca1⁺ VSCs migrate into the medial layer and generate *de novo* SMCs, which subsequently expand more efficiently compared with pre-existing smooth muscle. Genetic lineage tracing using dual recombinases distinguished a Sca1⁺PDGFR α ⁺ VSC subpopulation that generates SMCs, and genetic ablation of Sca1⁺ VSCs or specific knockout of Yap1 in Sca1⁺ VSCs significantly impaired artery repair. These findings provide genetic evidence of a *bona fide* Sca1⁺ VSC population that produces SMCs and delineates their critical role in vessel repair.

INTRODUCTION

The most prominent feature of arteries is the thick layer of smooth muscle that constitutes the majority of the cells of the vessel wall. Vascular smooth muscle cells (SMCs) in different

segments of arteries have several distinct origins in development. This heterogeneity may partially determine the site-specific location of vascular diseases and influence the progress of vascular diseases (Cheung et al., 2012). For example, SMCs in the aorta have at least three distinct cell sources in development. The SMCs colonizing the ascending aorta are derived partly from the secondary heart field and partly from the neural crest (Sawada et al., 2017; Waldo et al., 2005), SMCs populating the remaining arch are derived from the neural crest (Jiang et al., 2000), and SMCs residing in the descending aorta are derived from somatic mesoderm (Wasteson et al., 2008). In different kinds of vascular diseases, pathophysiological changes are prone to take place in certain regions, showing regional susceptibility of arteries to calcification (Leroux-Berger et al., 2011), aneurysm (Ruddy et al., 2008), and atherosclerosis (DeBakey et al., 1985; Bennett et al., 2016). The heterogenous cell origins of an artery may not only be manifested in the aorta but also in organ-specific arteries. For example, SMCs of coronary arteries have at least 2 important development origins: epicardium and endocardium (Pérez-Pomares et al., 1998; Gittenberger-de Groot et al., 1998; Dettman et al., 1998; Chen et al., 2016). The different cellular sources of SMCs may inform their distinct functions and propensity for certain vascular injuries or diseases.

During daily wear and tear, new SMCs are generated at a speed that compensates for loss of SMCs and maintains the proper function of arteries (Psaltis and Simari, 2015). Like developmental sources, SMCs in the adult stage may also have different cellular sources that continually fuel the pool of smooth muscle after their loss. At least four distinct sources have been proposed to generate new SMCs in the adult artery after injury (Majesky et al., 2011). First, cell division of pre-existing SMCs



is a major source of new SMCs, although this is not necessarily the exclusive source. Second, circulating hematopoietic stem cells from bone marrow have been proposed to differentiate into vascular SMCs during pathological remodeling of arteries (Saiura et al., 2001; Sata et al., 2002). However, later it was reported that pre-existing SMCs in the local artery wall, but not circulating progenitor cells from bone marrow, contributed to new SMCs during vascular pathological progress (Bentzon et al., 2006, 2007). Third, some distinct stem or progenitor cells residing in the medial layer of vessel walls could generate new SMCs in response to injuries. It has been reported that the medial layer harbors ABCG2⁺ side population cells that have the capability to differentiate into smooth muscle (Sainz et al., 2006). However, there is no direct *in vivo* evidence supporting the existence of side population cells for smooth muscle contribution. Recently, multipotent vascular stem cells residing in the medial layer have been proposed to generate smooth muscle during vascular remodeling and neointimal hyperplasia (Tang et al., 2012). However, this study lacks convincing *in vivo* lineage tracing evidence supporting the multipotent stem cell model, raising serious concerns in the field (Nguyen et al., 2013; Tang et al., 2013). Fate mapping studies showed that SMCs in the vascular neointima formation are derived from local pre-existing SMCs (Bentzon et al., 2006, 2007; Nemenoff et al., 2011). Although SMCs beget SMCs at the whole-population level, there is heterogeneity of SMCs in proliferation because a few medial SMCs may undergo extensive expansion and generate large clones of SMCs in neointima formation (Chappell et al., 2016; Jacobsen et al., 2017). Furthermore, recent studies have suggested that a discrete population of medial SMCs expressing CD146 emerges during embryonic development and continues to generate new SMCs in response to artery injuries (Roostalu et al., 2018). Vascular stem or progenitor cells in the adventitial layer of vessel wall have been proposed to contribute to SMCs in the neointima and atherosclerosis plaque (Hu et al., 2004). These pioneering studies of the SMC potential of Sca1⁺ cells mainly used cell transplantation approaches (Hu et al., 2004; Tsai et al., 2012) and *in vitro* cell culture assays (Passman et al., 2008). Interestingly, a subpopulation of adventitial Sca1⁺ progenitor cells could also be generated *in situ* from differentiated SMCs in the outer media, which represents the plasticity of pre-existing SMCs as a physiological program for maintaining stem cell pool (Majesky et al., 2017; Zhang and Xu, 2017). However, fate mapping results from SMC-inducible Cre drivers showed that, during vascular injuries, pre-existing SMCs mount a proliferative response and contribute to neointima formation and vascular wall remodeling (Bentzon et al., 2006, 2007; Nemenoff et al., 2011; Roostalu et al., 2018). Whether *bona fide* Sca1⁺ vascular stem cells (VSCs) exist *in vivo* has remained controversial and undetermined in the field for the past decade. Their putative role in vascular repair and regeneration is elusive and unknown.

In this study, we generated *Sca1-CreER* to fate-map Sca1⁺ cells in artery homeostasis and after injuries. We found that, after severe artery injury, Sca1⁺ cells generated *de novo* SMCs in the medial layer of vessel walls. Dual recombinase-mediated lineage tracing demonstrated that Sca1⁺PDGFRa⁺ VSCs in the adventitial mesenchyme contributed to these new SMCs for vascular repair. Of note, Sca1-derived SMCs

have more proliferation potential than pre-existing SMCs, generating more SMCs for full recovery of the vessel wall. Functionally, genetic ablation of Sca1⁺ VSCs or Yap1 deletion significantly impaired their contribution to SMCs for vessel repair and regeneration. Our work demonstrates that Sca1⁺ VSCs contribute to SMCs and play a critical role in vascular repair, representing a new potential therapeutic target for treating vascular diseases.

RESULTS

Single-Cell RNA Sequencing Analysis of Sca1⁺ Cells in the Artery Wall

To examine the cellular components of Sca1⁺ cells, individual cells were isolated from the femoral artery by enzymatic digestion and processed for single-cell RNA sequencing (scRNA-seq). scRNA-seq profiles were obtained from 5,353 cells, and, on average, 1,667 genes were detected per cell (Figures S1A and S1B). As shown, t-distributed stochastic neighbor embedding (t-SNE) analysis of this dataset revealed clusters of endothelial and adventitial cell populations (Fibr_Per1 cells (clusters 1–4) [Fibr_Per1_1–4]) based on marker gene expression (Figure 1A), with *Pecam1* marking endothelial cells and *PDGFRa* or *PDGFRb* artery adventitial cells (Figure 1B; Figures S1C and S1D). Further pathway enrichment analysis revealed that extracellular matrix organization-related pathways were enriched in adventitial cells (Fibr_Per1_1–4), indicating the function of these cells (Figure 1C). We noticed that *Sca1* was mainly expressed in adventitial cells and endothelial cells of arteries (Figure 1D). Adventitial cells expressing *PDGFRa* or *PDGFRb* could be further segregated into three distinct clusters based on the expression levels of *PDGFRa* and *PDGFRb* gene in the t-SNE map (Figures 1E and 1F), highlighting the heterogeneity of this population. Remarkably, among Sca1⁺ adventitial cells that also expressed *PDGFRa* or *PDGFRb*, 69% of them were *PDGFRa*-positive, and 20% were *PDGFRb*-positive (Figure 1G). Quantitative data also showed that 20.64% of all Fibr_Per1_1–4 cells shared the Sca1⁺PDGFRa⁺ profile. By using gene set enrichment analysis (GSEA) to characterize the function of each cell subpopulation, we identified that, compared with *PDGFRb*⁺ cells, several pathways were enriched in *PDGFRa*⁺ cells, including *BIOCARTA_ACTINY*, *PROTEASOME*, *PGC1A*, and *BIOCARTA_HDAC* pathways (Figure 1H; Figures S1E–S1H). Some of these pathways are known to regulate the differentiation, proliferation, and migration of SMCs (Yeligar et al., 2018; Barringhaus and Matsumura, 2007; Kapadia et al., 2009), indicating that *PDGFRa*⁺ and *PDGFRb*⁺ cells may have different properties and functional heterogeneity in vascular homeostasis or injuries.

To understand whether there is relevant heterogeneity in the Sca1⁺PDGFRa⁺ cell population and to estimate the differentiation potency of these cells, we performed further t-SNE analysis of double-positive cells from Fibr-Per1 clusters, which categorized Sca1⁺PDGFRa⁺ cells into four cell clusters (Figures S2A–S2C). Next, Markov chain entropy (MCE) values were computed to estimate the stemness of these four clusters. One-way ANOVA revealed that there were significant differences in differentiation potency among these four clusters (Figure S2D). Next we performed a multiple comparisons test, which indicated

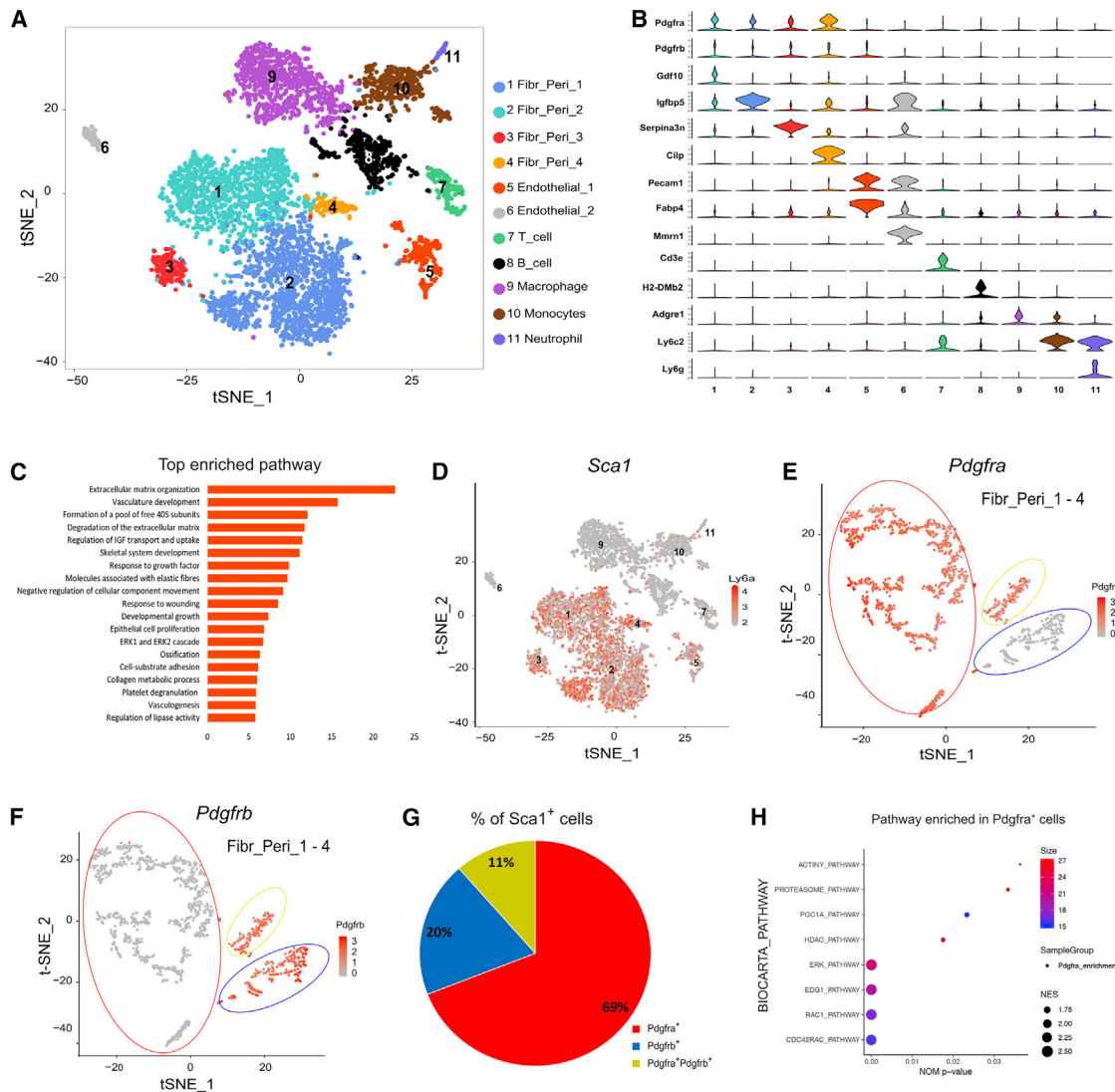


Figure 1. scRNA-seq Analysis of Femoral Artery Cells

- (A) Visualization of unsupervised clustering in a t-distributed stochastic neighbor embedding (t-SNE) plot of 5,353 cells isolated from a femoral artery.
 (B) Violin plots showing the expression levels of representative marker genes across the 11 clusters.
 (C) Top enriched pathway of unique genes in Fibr_Per1_1–4.
 (D) Distribution of *Sca1* across all subpopulations.
 (E and F) Gene expression levels of *Pdgra* (E) or *Pdgrfb* (F) in a t-SNE map of Fibr_Per1_1–4 cells (PDGFRa⁺ or PDGFRb⁺ populations) with supervised clustering.
 (G) The percentage of Sca1⁺ cells expressing *Pdgra*, *Pdgrfb*, or both. Sca1⁺PDGFRa⁺ or Sca1⁺PDGFRb⁺ cells from Fibr_Per1_1–4 were analyzed.
 (H) Images showing pathways significantly enriched in Pdgra⁺ cells using BioCarta gene sets for GSEA ($p < 0.05$).

that clusters 1 and 4 have a higher differentiation potential than clusters 2 and 3. To further confirm these observations, we also performed GSEA using a stemness gene signature defined previously (Ramalho-Santos et al., 2002). The stemness-related gene signature was significantly enriched in cluster 1 compared with the other three clusters. Collectively, by two analysis methods, MCE and GSEA, for analysis of stemness of different clusters, cluster 1 was estimated to have more potential as stem cells (Figure S2E). Whether these four populations have the same propensity to differentiate into SMCs requires more sophisticated genetic tools to distinctly label them for fate mapping studies in the future.

We also examined previously reported adventitial progenitor cell markers such as CD34, CD45, c-Kit, c-Myb, and Klf4. We found that CD34 and Klf4 expression was high in Fibr_Per1 cells (clusters 1–4) and endothelial_1 cells (cluster 5), which were highly associated with *Sca1* expression (Figure S3A). CD45 was highly expressed in immune-related cells such as T cells, B cells, macrophages, monocytes, and neutrophils. Most cells expressing CD146 (*Mcam*) were Endothelial_1 cells, the endothelial cell population that also expresses high *Sca1*. Very rarely, cells expressed c-Kit, and we did not detect c-Myb in our scRNA sequencing data (Figure S3A).

Characterization of Sca1⁺ Cells in the Femoral Artery

To reveal the positional information of Sca1-expressing cells in the vessel walls of adult mice (8 weeks old at the start of each experiment), we generated a genetic lineage tracing system for Sca1⁺ cells by crossing *Sca1-CreER* with *R26-tdTomato* mouse lines (Figure 2A). To examine Sca1⁺ cells in the vessel wall, we treated *Sca1-CreER;R26-tdTomato* mice with tamoxifen (Tam) and collected tissue samples within 24–48 h for analysis, when the tdTomato reporter represented Sca1-expressing cells (Figure 2B). We could readily detect tdTomato fluorescence in whole-mount artery samples after Tam treatment (Figure 2C). Immunostaining for tdTomato and Sca1 on dissociated cells isolated from arteries showed that 75.38% ± 3.19% of Sca1⁺ cells express tdTomato (Figure 2D), indicating a high efficiency of cell labeling by *Sca1-CreER*. Flow cytometric analysis showed that 75.16% ± 1.80% of Sca1⁺ cells were labeled with tdTomato, whereas over 95% of tdTomato⁺ cells expressed Sca1 (Figure 2E), indicating a high efficiency and specificity of *Sca1-CreER* for lineage tracing of Sca1⁺ cells. These data demonstrated that the tdTomato signal faithfully represented Sca1⁺ cells. To examine the detailed cell types labeled by Sca1 in the tissue, we sectioned femoral arteries for immunostaining of tdTomato and cell lineage markers. We found that a subset of tdTomato⁺ cells in the adventitial layer were colocalized with PDGFRa or PDGFRb (Figures 2F and 2H). Quantitatively, by immunostaining, 40.84% ± 1.86% and 11.46% ± 1.73% of tdTomato⁺ cells expressed PDGFRa and PDGFRb, respectively (Figure 2F). The tdTomato staining was specific because we did not detect it in tissue collected from oil-treated *Sca1-CreER;R26-tdTomato* mice (Figure 2G). Flow cytometry analysis of cells isolated from arteries showed that ~40% and ~10% of tdTomato⁺ cells in the vessel walls were PDGFRa⁺ and PDGFRb⁺, respectively (Figures 2H and 2I). Sectional staining of the hematopoietic cell marker CD45 and endothelial cell marker CDH5 showed that 0% and 40.04% ± 2.58% of tdTomato⁺ cells were CD45⁺ and CDH5⁺, respectively (Figure 2J). This was confirmed by flow cytometry analysis (Figure 2K). We also noticed that a subset of adipose tissue outside of the vessel wall was tdTomato⁺ (Figure 2L). By using four conventional smooth muscle markers (Majesky et al., 2011), we did not detect any tdTomato⁺ cells expressing smooth muscle-calponin (CNN1), alpha smooth muscle actin (SMA), smooth muscle myosin heavy chain (SM-MHC), or smooth muscle 22 alpha (SM22) in tissue sections examined (over 250 sections from 5 mice; Figures 2M–2O). We showed that Sca1⁺ cells constituted endothelial cells in the intima layer and adventitial stromal cells in the vessel wall and a subset of adipocytes surrounding vessels (Figure 2P). Sca1 was not expressed by smooth muscle or hematopoietic cells in the vessel wall (Figure 2P).

Sca1⁺ Cells Do Not Contribute to SMCs during Homeostasis or after Wire-Injury

We next examined whether Sca1⁺ cells generated new SMCs during tissue homeostasis or after vascular injuries. We collected mouse tissues 8–12 weeks after Tam treatment (Figure 3A). Immunostaining for tdTomato, SM-MHC, and CDH5 showed that labeled cells maintained an endothelial cell fate but did not contribute to smooth muscle (Figure 3B). Flow cytometry analysis confirmed endothelial cell but not smooth muscle cell fate

(Figure 3C). Immunostaining for SMA and SM22 validated that the vessel wall was devoid of tdTomato⁺ SMCs during normal homeostasis (Figures 3D and 3E). Labeled cells were also residing in the adventitial layer of the vessel wall, and a subset of them expressed PDGFRa or PDGFRb (Figures 3F and 3G). Flow cytometry analysis of the labeled cells showed that ~40% and 10% of tdTomato⁺ cells expressed PDGFRa and PDGFRb, respectively (Figures 3H and 3I). These data demonstrate that Sca1⁺ cells maintain original cell fates during vascular homeostasis.

We next performed wire-induced vessel injury and analyzed tissue samples 4 weeks after injury (Figure 3J). H&E staining showed neointima formation after wire injury compared with a normal artery as a sham control (Figure 3K). Immunostaining for SM-MHC, CNN1, SM22, and SMA on tissue sections showed that the vessel wall was devoid of tdTomato⁺ SMCs after wire injury (Figures 3L–3N). Flow cytometry analysis confirmed that Sca1⁺ cells did not contribute to SMCs after injury (Figure 3O). Instead, Sca1⁺ cells in the intimal layer maintained CDH5⁺ endothelial cell fate (Figure 3M). We detected tdTomato⁺PDGFRa⁺ adventitial stromal cells but not tdTomato⁺CD45⁺ hematopoietic cells in the vessel wall (Figure 3P). We also found that a subset of Sca1⁺ cells in the adventitial layer proliferated after wire injury (Figure 3Q). We also performed *SM22-CreER* lineage tracing on injury and sham models and found that virtually all SMCs in the injured vessel were derived from pre-existing SMCs (Figure S4), which was consistent with previous work (Bentzon et al., 2006, 2007; Nemenoff et al., 2011). Taken together, Sca1⁺ cells did not contribute to SMCs in homeostasis or after wire injury (Figure 3R).

Sca1⁺ Cells Generate De Novo SMCs after Severe Vessel Injury

We next wanted to find out whether the SMC differentiation potential of Sca1⁺ cells could be activated under severe injury conditions. To induce severe vessel injury, we used an arterial anastomosis model that involves full *trans*-sectional injury to the arterial wall with loss of local SMCs and subsequent regeneration of the arterial SMC layer to heal the anastomosis site (Roostalu et al., 2018; Perlman et al., 1997). We performed the procedure 2 weeks after Tam treatment and collected tissue samples after 2 weeks (short term) and 5 weeks (long term) (Figure 4A). We segmented the femoral artery into 4 zones according to their position relative to the site of anastomosis and their morphology after injury (Figure 4B). Zone 1, which was distal to the site of anastomosis, had normal morphology. Zone 2 encompassed the anastomosis site. Zones 3 and 4 were proximal to the site of anastomosis; zone 3 had disorganized SMCs, and zone 4 had a normal arterial morphology that was indistinguishable from a healthy artery (Figure 4C), consistent with previous descriptions (Roostalu et al., 2018). We observed brighter tdTomato⁺ signals from the anastomosed vessel segment compared with sham controls (Figure 4D), which was consistent with expansion of the Sca1⁺ population, as indicated by 5-ethynyl-2'-deoxyuridine (EdU) incorporation in tdTomato⁺ cells (Figure 4E). Immunostaining for SMA and tdTomato in zone 1 to zone 4 vessel segments showed that only zone 2 hosted tdTomato⁺ SMCs in the medial layer of vessel wall (Figure 4F). Quantitatively, 13.16% ± 1.17% of SMCs in zone 2 were derived from Sca1⁺ cells

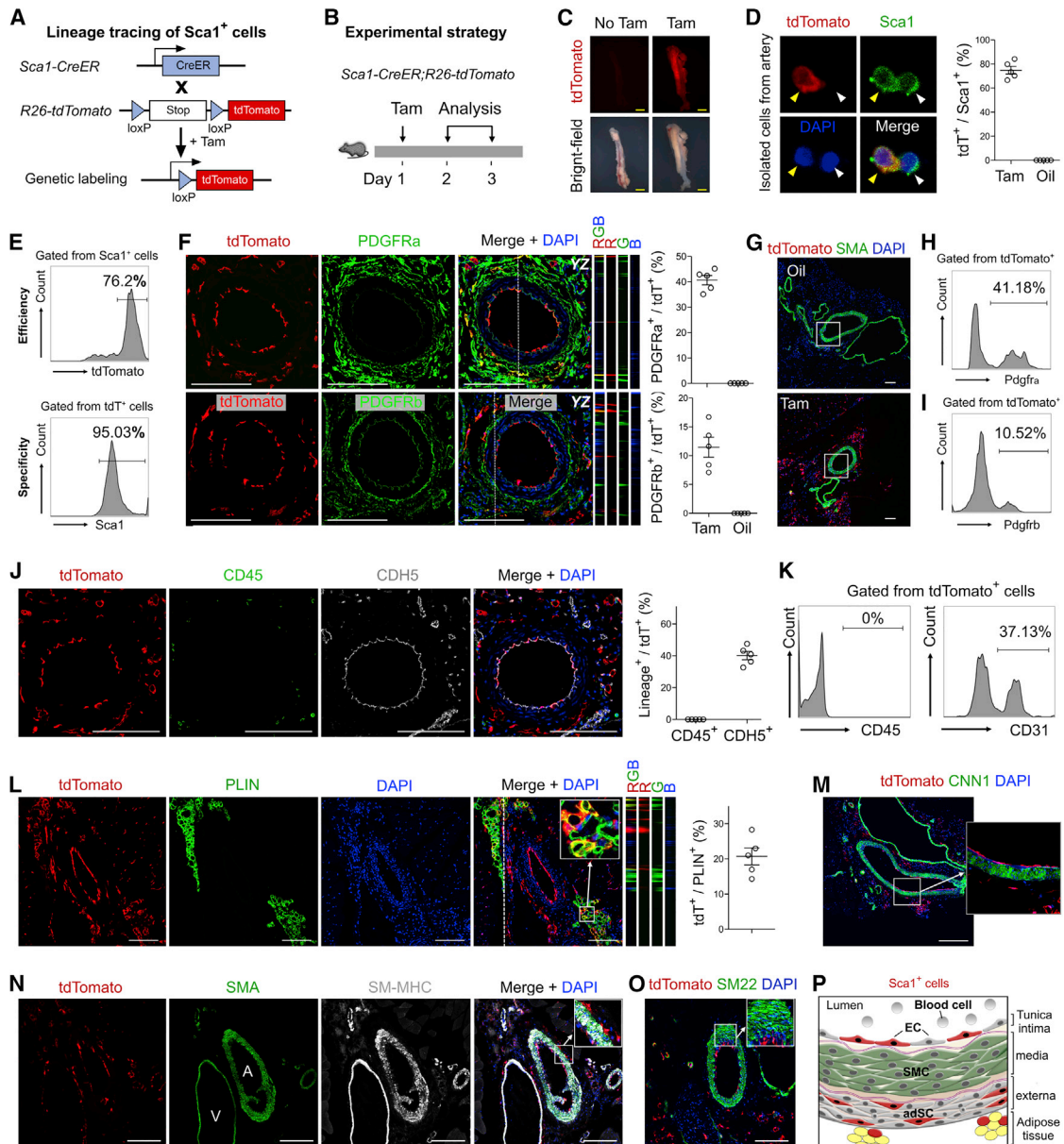


Figure 2. Characterization of $Sca1^{+}$ Cells in an Artery

(A) Schematic showing genetic lineage tracing by *Sca1-CreER*.

(B) Sketch of the experimental design.

(C) Fluorescence and bright-field images of aortae from *Sca1-CreER;R26-tdTomato* mice treated with or without Tam.

(D) Immunostaining for tdTomato and Sca1 on isolated cells from a femoral artery and quantification of the percentage of tdTomato⁺ cells in Sca1⁺ cells. Data are mean \pm SEM; n = 5.

(E) Flow cytometry analysis of the labeling efficiency and specificity of $Sca1^{+}$ cell labeling.

(F) Immunostaining for tdTomato and PDGFRa or PDGFRb on femoral artery sections. The dotted line indicates signals from the yz axis on z stack images. Right panel: quantification of the percentage of PDGFRa⁺ or PDGFRb⁺ cells in tdTomato⁺ (tdT⁺) cells.

(G) Immunostaining for tdTomato and SMA on tissue sections of *Sca1-CreER;R26-tdTomato* mice treated with oil or Tam.

(H and I) Flow cytometry analysis of the percentage of PDGFRa⁺ (G) and PDGFRb⁺ (I) cells in tdT⁺ cells.

(J) Immunostaining for tdTomato, CD45, and CDH5 on an artery section and quantification of CDH5⁺ and CD45⁺ cells in tdT⁺ cells.

(K) Flow cytometry analysis of the percentage of CD45⁺ and CD31⁺ cells in tdT⁺ cells.

(L) Immunostaining for tdTomato and PLIN on an artery section and quantitation of the labeled PLIN⁺ cells by *Sca1-CreER*. Inset: magnification of the boxed region.

(M–O) Immunostaining for tdTomato, CNN1 (M), SMA, SM-MHC (N), and SM22 (O) on tissue sections.

(P) Cartoon image showing that $Sca1^{+}$ cells include a subset of endothelial cells (ECs), adventitial stromal cells (adSCs) that include PDGFRa⁺ or PDGFRb⁺ cells, and adipocytes but not smooth muscle cells (SMCs).

Scale bars, 1 mm (yellow) and 100 μ m (white).

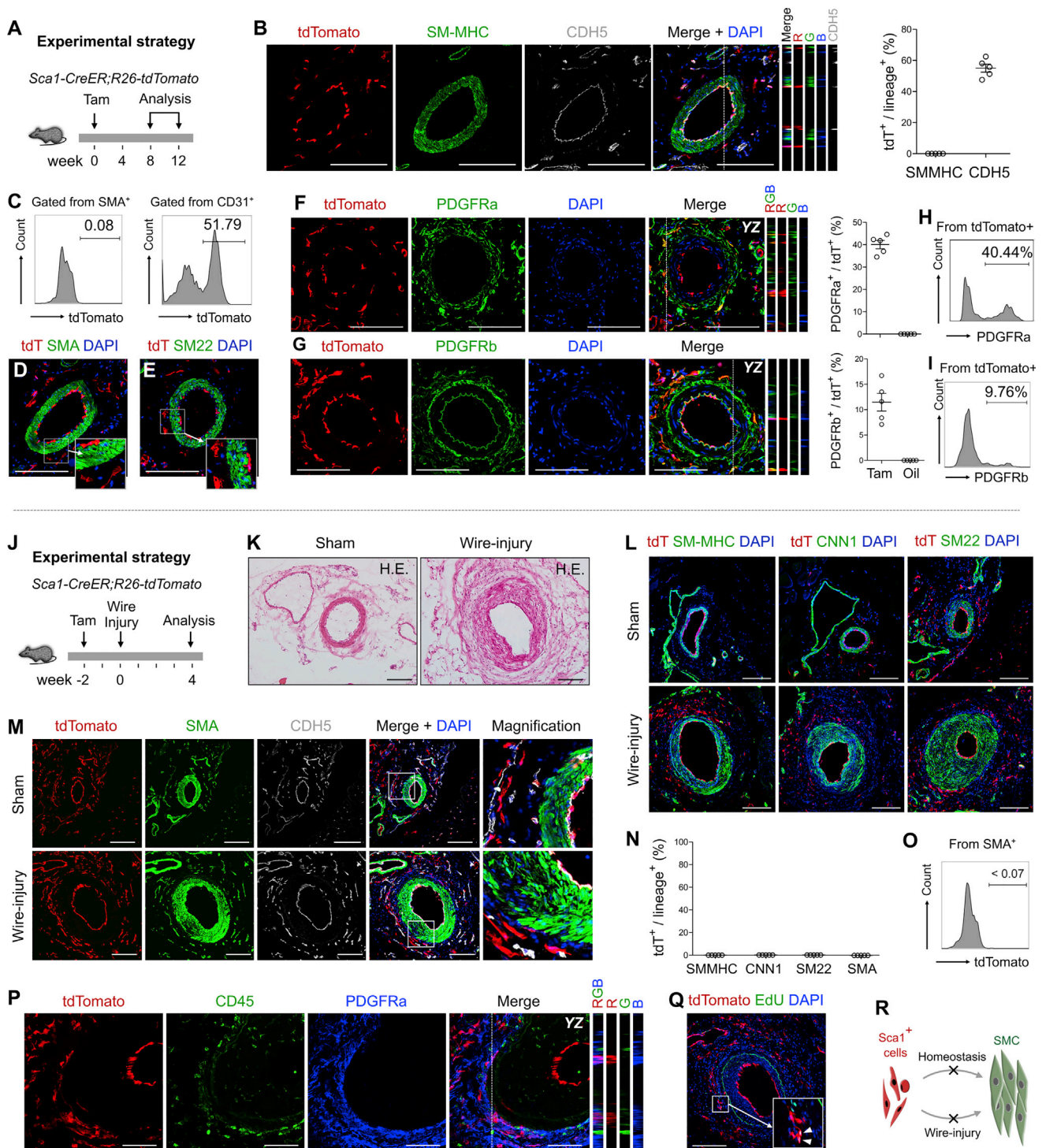


Figure 3. Sca1⁺ Cells Do Not Contribute to SMCs during Homeostasis or after Wire Injury

(A) Schematic showing the experimental strategy.
 (B) Immunostaining for tdTomato, SM-MHC, and CDH5 on a femoral artery section and quantification of the percentage of SM-MHC⁺ cells or CDH5⁺ cells expressing tdTomato. Data are mean ± SEM; n = 5.
 (C) Flow cytometry analysis of the percentage of SMA⁺ or CD31⁺ cells expressing tdTomato.
 (D and E) Immunostaining for tdTomato (tdT) and SMA (D) or SM22 (E) on tissue sections.
 (F and G) Immunostaining for tdTomato and PDGFRa (F) or PDGFRb (G) on tissue sections. Right panels: quantification of the percentage of tdTomato⁺ cells that express PDGFRa or PDGFRb.
 (H and I) Flow cytometric analysis of tdTomato⁺ cells that express PDGFRa (H) or PDGFRb (I).
 (J) Experimental strategy for wire injury, with Tamoxifen at week -2, wire injury at week 0, and analysis at week 4.
 (K) Histology (H.E.) of Sham and Wire-injury arteries.
 (L) Immunostaining for tdTomato and SM-MHC, CNN1, or SM22.
 (M) Immunostaining for tdTomato, SMA, and CDH5 in Sham and Wire-injury conditions, with magnification views.
 (N) Quantification plot showing 0% tdT⁺/lineage⁺ for SMMHC, CNN1, and SM22.
 (O) Flow cytometry analysis of SMA⁺ cells (<math>< 0.07\%</math>).
 (P) Immunostaining for tdTomato, CD45, and PDGFRa.
 (Q) Immunostaining for tdTomato, EdU, and DAPI.
 (R) Schematic diagram showing that Sca1⁺ cells do not contribute to SMCs during homeostasis or after wire injury.

(legend continued on next page)

(Figure 4G). In parallel, we performed *SM22-CreER*-mediated lineage tracing and found a significant dilution in the labeling percentage of SMCs in zone 2 after injury (Figure S5), indicating that some of the SMCs that heal transactional injury were derived from new sources rather than from pre-existing SMCs. Of note, *Sca1*-derived cells expressed CNN1 and SM22 but not SM-MHC (Figures 4H–4J). Because SM-MHC (Myh11) is a marker for mature SMCs (Cherepanova et al., 2016), these newly formed SMCs did not fully acquire the mature SMC phenotype within the first 2 weeks (Figure 4K).

We then collected tissue samples at later stages (5 weeks) after severe injury and examined their morphology by H&E to distinguish zone 1 to zone 4 (Figure 4L). Flow cytometry analysis of dissociated vascular cells from zone 2 of injured vessels showed that $9.07\% \pm 1.15\%$ of SMCs were tdTomato⁺ compared with 0% in the sham control (Figure 4M). By immunostaining of tissue sections, we again found tdTomato⁺SMA⁺ SMCs in zone 2 (Figure 4N), which constituted $14.3\% \pm 1.46\%$ of the SMCs in the vessel wall (Figure 4O). These tdTomato⁺ cells expressed SM22, CNN1, and SM-MHC in the medial layer, indicating acquisition of the fully mature SMC phenotype 5 weeks after injury (Figures 4P–4R). Additionally, we detected EdU incorporation in tdTomato⁺ SMCs and also expansion of tdTomato⁺ stromal cells in the adventitial layer (Figures 4S and 4T). These data demonstrated that *Sca1*-derived cells contributed to mature SMCs in the medial layer 5 weeks after severe injury (Figure 4U).

Sca1⁺PDGFRa⁺ but Not Sca1⁺PDGFRb⁺ VSCs Generated SMCs

Single-cell RNA sequencing (Figure 1) and genetic cell labeling data (Figure 2) showed that *Sca1*⁺ cells were a heterogeneous population that included endothelial cells, adipocytes, hematopoietic cells, and adventitial stromal cells expressing PDGFRa or PDGFRb (Figure 2P). It was intriguing to explore which type of *Sca1*⁺ cells actually generated new SMCs. To systematically examine cell lineages, we first used the *Cdh5-CreER*, *Fabp4-Cre*, and *CD45-Dre* drivers to trace CDH5⁺ cells, PLIN⁺ adipocytes, and CD45⁺ hematopoietic cells, respectively, after severe vessel injury (Figures 5A–5C). We found that these labeled cells maintained their original cell phenotypes without contributing to SMCs (Figures 5A–5C; Figure S6), excluding endothelial cells, adipocytes, and hematopoietic cells as potential cell sources for generating new SMCs after injury.

Because stromal cells in the adventitial layer were mainly composed of PDGFRa⁺ and PDGFRb⁺ cell populations (Figures 1 and 2F–2I; Figure S1), we employed an intersectional genetics strategy (Zhang et al., 2016b; Liu et al., 2019) by using dual recombinase-based lineage tracing to fate-map these two specific

sub-populations of *Sca1*⁺ cells. We first combined *PDGFRa-DreER* and *Sca1-CreER* with the *R26-RSR-LSL-tdTomato* reporter (short for *R26-rox-stop-rox-loxp-stop-loxp-tdTomato*) for lineage tracing of PDGFRa⁺*Sca1*⁺ cells (Figure 5D). Only after both *Dre-rox* and *Cre-loxP* recombination could the tdTomato reporter be expressed in PDGFRa⁺*Sca1*⁺ cells residing in the adventitial layer (Figure 5D). We did not detect any tdTomato⁺ SMCs in vessels from mice without injury (Figure 5E). In the injured vessel, however, we found a subset of tdTomato⁺ cells in the medial wall that co-expressed the SMC markers SMA, SM22, CNN1, and SM-MHC (Figures 5F–5H), demonstrating that PDGFRa⁺*Sca1*⁺ VSCs generated SMCs during healing of the anastomosis site. Because dual recombinase-mediated lineage tracing depends on both inducible *CreER* and *DreER*, the efficiency would be lower than for single lineage tracing; e.g., by *Sca1-CreER*-mediated cell labeling. Therefore, tdTomato⁺ cells labeled by *Sca1-CreER*; *Pdgfra-DreER* were fewer and regional on the vessel wall (Figures 5F–5I) compared with those labeled by the *Sca1-CreER* tracer.

To address whether PDGFRb⁺*Sca1*⁺ cells differentiated into SMCs after injury, we generated a new strategy employing a sequential intersectional genetics (Pu et al., 2018) by which *Sca1-CreER* expression leads to *Dre* expression under the PDGFRb gene promoter (Figure 5J). Combination with the *R26-RSR-tdT* reporter (short for *R26-rox-stop-rox-tdTomato*) secures tdTomato expression exclusively in *Sca1*⁺PDGFRb⁺ cells upon Tam injection (Figure 5J). Immunostaining for tdTomato and PDGFRb on tissue sections from *Sca1-CreER*; *Pdgfrb-LSL-Dre*; *R26-RSR-tdTomato* and *Sca1-CreER*; *R26-tdTomato* mice showed that the labeling efficiency was comparable between the two groups (Figures 5K and 5L). We used the same anastomosis model and collected tissue samples 5 weeks after injury for analysis (Figure 5M). Although we did observe neointima formation after severe injury in zone 2 (Figure 5N), we could not detect any tdTomato⁺ cells expressing SMA, SM22, SM-MHC, or CNN1 in any of the 250 sections examined from 5 mice (Figure 5O). Taken together, among different mesenchymal cell populations, we pinpointed that adventitial *Sca1*⁺ VSCs expressing PDGFRa are capable of generating *de novo* smooth muscle for vascular repair and regeneration (Figure 5P).

Sca1-Derived SMCs Were More Competent to Expand for Full Recovery

To assess the ultimate contribution in the fully repaired vessel, we collected tissue samples 12–24 weeks after injury (Figure 6A). Flow cytometry analysis of dissociated cells from the vessel wall around the healed anastomosis site (zone 2) showed that $21.72\% \pm 2.32\%$ SMCs expressed tdTomato (Figures 6B and

(J) Schematic showing the experimental strategy. Wire injury was induced 1 week after Tam induction.

(K) H&E staining of a femoral artery after sham or wire injury.

(L) Immunostaining for tdT and the smooth cell markers SM-MHC, CNN1, and SM22 on tissue sections of femoral arteries from sham or wire injured mice.

(M) Immunostaining for tdTomato, SMA, and CDH5 on tissue section.

(N) Quantification of the percentage of tdTomato⁺ cells expressing SMA and CDH5.

(O) Flow cytometry analysis of SMA expression in tdTomato⁺ cells.

(P) Immunostaining for tdTomato, CD45, and PDGFRa on tissue section.

(Q) Immunostaining for tdTomato and EdU on tissue sections.

(R) Cartoon image showing that *Sca1*⁺ cells do not generate SMCs during homeostasis or after wire injury.

Scale bars, 100 μ m.

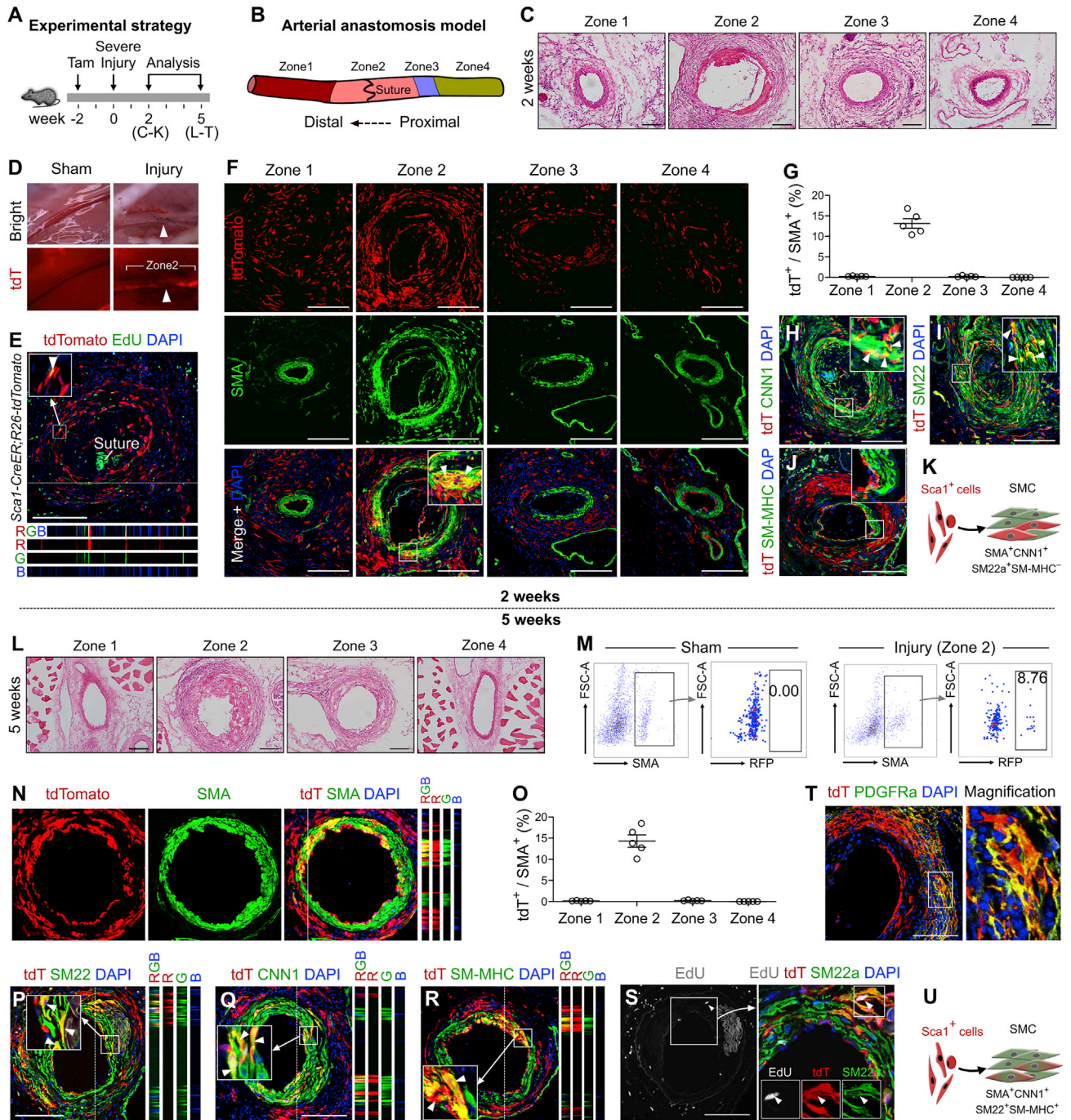


Figure 4. Sca1⁺ Cells Differentiate into SMCs during Arterial Anastomosis

(A) Schematic showing the experimental strategy.
 (B) Cartoon image showing the arterial anastomosis model.
 (C) H&E staining on arterial sections of zones 1–4.
 (D) Whole-mount fluorescence and bright-field images of a femoral artery. Arrowheads indicate sutures.
 (E) Immunostaining for tdTomato and EdU on arterial sections, showing EdU⁺tdTomato⁺ cells (arrowheads).
 (F) Immunostaining for tdTomato and SMA on zones 1–4 of arterial sections. Arrowheads indicate SMA⁺tdTomato⁺ cells.
 (G) Quantification of the percentage of SMA⁺ cells that express tdTomato. Data are mean ± SEM; n = 5.
 (H–J) Immunostaining for tdTomato and CNN1 (H), SM22 (I), and SM-MHC (J) on arterial sections, showing that a subset of tdTomato⁺ cells express CNN1 or SM22a (arrowheads) but not SM-MHC.
 (K) Cartoon image showing that Sca1⁺ cells contribute to immature SMC after injury.
 (L) H&E staining on arterial sections of zones 1–4.

(legend continued on next page)

6C). Because the exact demarcation of zone 2 was not clear after full repair, it is possible that border regions of the neighboring zones (e.g., zone 1 or zone 3) were included in the digested tissue, which could lead the flow cytometry assay to underestimate the significant contribution of Sca1⁺ cells to SMCs at the critical anastomosis site. We therefore performed immunostaining on sections of zone 2 and found that a significant portion of cells expressing SMA, SM22, CNN1, and SM-MHC were tdTomato⁺ in the anastomosis region (Figures 6D–6F and 6H). Quantitatively, 30.32% ± 2.32% of CNN1⁺ SMCs and 30.62% ± 2.77% of SM-MHC⁺ SMCs in zone 2 expressed tdTomato (Figures 6G and 6I), indicating that they were derived from Sca1⁺ VSCs. Such cells were not found in zones 1, 3, or 4 (Figure S7). Of note, significantly more tdTomato⁺ SMCs (21.52% ± 1.32%) incorporated EdU than tdTomato⁻ SMCs (16.92% ± 1.08%) in the same tissue sections (Figure 6J), indicating that Sca1-derived SMCs expand more than pre-existing SMCs during vessel recovery. These data indicate that PDGFRa⁺Sca1⁺ VSCs give rise to SMCs that are more competent to proliferate during regeneration of the arterial media at the anastomosis site (Figure 6K).

Deletion of Sca1⁺ VSCs or Yap1 Knockout Impaired Vessel Repair

To functionally address the role of Sca1⁺ VSCs in vessel repair and regeneration, we crossed the *Sca1-CreER;R26-tdTomato* and *R26-DTR* mouse lines (Buch et al., 2005) to allow selective ablation of the Sca1⁺ cell population at the time point of choice (Figure 7A). Addition of diphtheria toxin (DT) leads to its binding with the diphtheria toxin receptor (DTR), specifically expressed on Sca1⁺ cells, resulting in termination of protein synthesis and, thus, apoptotic death of DTR-expressing cells (Naglich et al., 1992). We treated mice with Tam and then DT before performing arterial anastomosis, with each procedure separated by a 2 weeks interval, and then analyzed tissues at 2–8 weeks of arterial repair (Figure 7B). As a control for DT-mediated cell ablation, we used *Sca1-CreER;R26-DTR/tdTomato* mice treated with PBS instead of DT. We found that DT-treated *Sca1-CreER;R26-DTR/tdTomato* mice had significantly fewer tdTomato⁺ cells in the adventitial layer (Figures 7B and 7C), and the healed medial layer was devoid of tdTomato⁺ SMCs, in contrast to healed arteries in *Sca1-CreER;R26-DTR/tdTomato* mice without DT treatment (Figure 7C). The thickness of the smooth muscle layer in zone 2 was significantly reduced in some regions compared with *Sca1-CreER;R26-DTR/tdTomato* samples without DT treatment (Figure 7C,D). It should be noted that other Sca1⁺ cells, such as endothelial cells and adipocytes, would also be targeted by DT treatment. Nevertheless, these data suggest that Sca1⁺ cells are critical for smooth muscle contribution and vessel wall structure normalization during vessel repair and regeneration.

Previous studies have shown that the Hippo signaling pathway regulates SMC proliferation during cardiovascular development (Wang et al., 2014; Osman et al., 2019). Sca1-derived SMCs expanded more significantly than pre-existing SMCs during injury recovery. We therefore examined whether the key co-transcriptional factor YAP was involved in expansion of Sca1-derived SMCs. By immunostaining for YAP and SMA on *Sca1-CreER;R26-tdTomato* artery sections, we found that YAP was enriched in tdTomato⁺ SMCs in zone 2 (Figure 7E), indicating that the Hippo pathway might be activated and important for regulating the contribution of Sca1-derived cells in vessel repair. To directly address this, we crossed *Sca1-CreER;R26-tdTomato* with *Yap1^{fl/fl}* mice (Schlegelmilch et al., 2011) to generate *Sca1-CreER;Yap1^{fl/fl};R26-tdTomato* to knock out YAP1 specifically in Sca1⁺ cells (mutant) and used littermates with the *Sca1-CreER;Yap1^{fl/+};R26-tdTomato* genotype as a control (Figure 7F). Immunostaining for YAP1 and tdTomato in zone 2 of healed arteries at 5 weeks in *Sca1-CreER;Yap1^{fl/fl};R26-tdTomato* mice showed that YAP was deleted in most tdTomato⁺ SMCs (Figure 7G). We could barely detect tdTomato⁺ SMCs incorporating EdU in the injured vessel wall (Figure 7H), and immunostaining for tdTomato and SMA on tissue sections showed that the percentage of Sca1-derived SMCs was significantly reduced in the mutant compared with the control (Figures 7I and 7J). By immunostaining for SM22, CNN1, and SM-MHC, we confirmed reduced Sca1-derived SMCs in the vessel wall (Figure 7J and data not shown).

Finally, we exposed mice for long-term tracing and collected tissue samples for analysis 20 weeks after the start of experiments (Figure 7K). Immunostaining for tdTomato and SM-MHC on tissue sections revealed that a substantial portion of SMCs expressed tdTomato in the control artery (31.76% ± 1.99%), whereas significantly fewer tdTomato⁺ SMCs were detected in the *Yap1* mutant artery (Figures 7L and 7M). By measuring smooth muscle cell layers, we found that the thickness of the artery wall was significantly reduced in the *Yap1* mutant compared with the control in the long-term post-injury period (Figure 7N). Taken together, these data demonstrate that YAP is required for incorporation and expansion of Sca1-derived SMCs in vascular repair and regeneration.

DISCUSSION

In this study, we used single-cell RNA sequencing and genetic lineage tracing to uncover the direct involvement of Sca1⁺ progenitor cells in remodeling and repair of severe vascular injury. We found that Sca1⁺ cells in the vessel wall are a heterogeneous population that consists of endothelial cells, peri-vascular adipocytes, and PDGFRa⁺ or PDGFRb⁺ stromal cells. An intersectional genetics strategy pinpointed the Sca1⁺PDGFRa⁺ cell

(M) Flow cytometry analysis of the percentage of SMA⁺ cells that express tdTomato in the sham or injury group.

(N) Immunostaining for tdT and SMA on tissue sections.

(O) Quantification of the percentage of SMA⁺ cells expressing tdTomato.

(P–R) Immunostaining for tdT and SM22 (P), CNN1 (Q), and SM-MHC (R).

(S) Immunostaining for EdU and a magnified region showing EdU⁺tdT⁺SM22⁺ cells (arrowheads).

(T) Immunostaining for tdTomato and PDGFRa on tissue sections.

(U) Cartoon image showing the contribution of Sca1⁺ cells to mature SMCs 5 weeks after injury.

Scale bars, 100 μm.

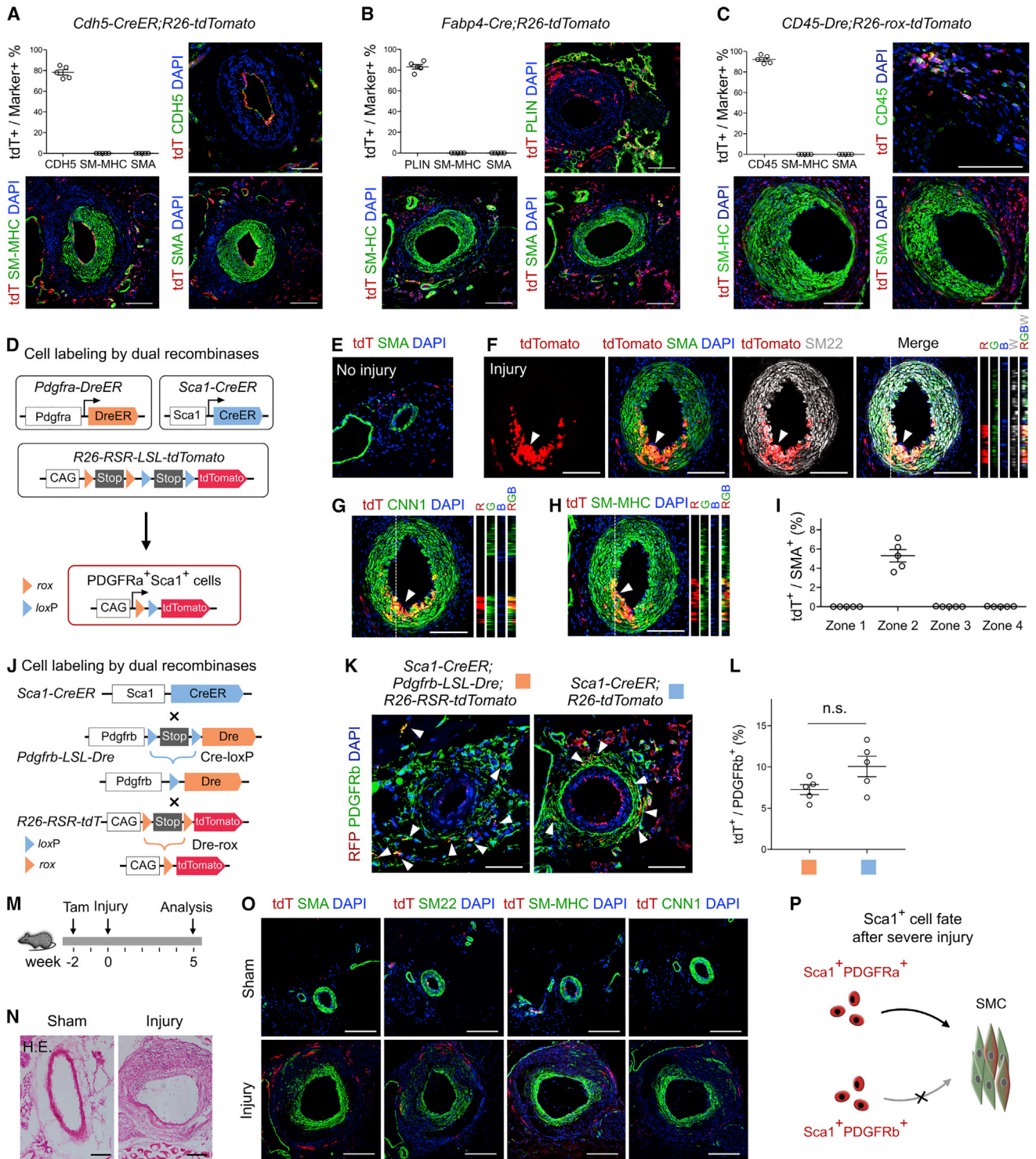


Figure 5. PDGFR α ⁺Sca1⁺ Cells Generate New SSMCs during Arterial Anastomosis

(A–C) Immunostained images of arteries collected from *Cdh5-CreER* (A), *Fabp4-Cre* (B), or *CD45-Dre* (C) lineage tracing mice, showing highly efficient labeling of each cell lineage, but they do not contribute to SMCs.

(D) Schematic showing strategy for labeling PDGFR α ⁺Sca1⁺ cells by dual recombinases-mediate intersectional genetic approach.

(E) Immunostaining for tdT and SMA on tissue sections (no injury).

(F–H) Immunostaining for tdTomato and SMA, SM22 (F), CNN1(G), or SM-MHC (H) on artery sections after injury. Arrowheads, tdTomato⁺ SMCs.

(I) Quantification of the percentage of SMA⁺ cells expressing tdTomato.

(J) Schematic diagram showing the genetic approach for labeling PDGFR β ⁺Sca1⁺ cells.

(legend continued on next page)

population as the source of *de novo* smooth muscle healing of severe transversal arterial injury. These Sca1⁺ VSC derived SMCs possessed more propensity to expand compared with pre-existing SMCs, imparting them an important fraction of SMCs regeneration. Genetic Sca1⁺ cell ablation and Yap1 gene deletion in Sca1⁺ cells indicated their involvement in vessel repair and recovery. Elucidation of this new cellular source for generating SMCs in vascular injury adds to our understanding of the physiology and pathophysiology of arteries and may also provide avenues for future therapeutic interventions for vascular diseases.

Sca1⁺ cells in the adventitial layer of the vessel wall were first proposed to be stem cells for smooth muscle more than a decade ago (Hu et al., 2004). Isolated Sca1⁺ cells could differentiate into SMCs after stimulation with platelet-derived growth factor BB (PDGF-BB) *in vitro* (Hu et al., 2004). Because of technical limitations at that time, genetic lineage tracing was not performed to understand the *in vivo* function of Sca1⁺ cells in vascular injury and remodeling. Instead, cultured Sca1⁺ cells from *SM-LacZ* transgenic mice were seeded in large numbers on irradiated vein grafts in mice, and some of the transplanted β -gal⁺ cells were found to contribute to SMCs in the developing neointima (Hu et al., 2004). Although these experiments showed the differentiation potential of the transplanted cells, they could not infer a physiological function of the adventitial Sca1⁺ population. First, the irradiation prevented proliferation of local vein SMCs, giving the transplanted Sca1⁺ cells an important competitive advantage. Second, the transplanted Sca1⁺ cells differed in number and, potentially, also in phenotype from endogenous Sca1⁺ cells. In the absence of *in vivo* Sca1⁺ stem cell lineage tracing experiments, the hypothesis of a regenerative function of Sca1⁺ cells in vascular biology has remained debated and unresolved. Indeed, it is well known that transplantation experiments and direct *in vivo* lineage tracing may lead to different, sometimes even contradictory conclusions. For example, transplantation of mammary basal progenitor cells supports its bi-potency for generating both luminal and basal components of mammary epithelium. However, lineage tracing studies showed that basal cells are uni-potent and generate basal but not luminal cells *in vivo* (Van Keymeulen et al., 2011). Transplantation of c-Kit⁺ cardiac or lung stem cells regenerates injured myocardium or lung, respectively, whereas lineage tracing data did not support these conclusions (Beltrami et al., 2003; van Berlo et al., 2014; Kajstura et al., 2018; Liu et al., 2015). SMC lineage tracing studies have shown that pre-existing SMCs play a major role in the accumulation of intimal SMCs in vascular pathologies but have not ruled out a potential contribution of other, still unknown sources in the vascular wall (Bentzon and Majesky, 2018; Nemenoff et al., 2011). Interestingly, a recent study using *Myh11-CreER* SMC lineage tracing showed that the fraction of SMCs originating from pre-existing SMCs was significantly diluted after severe transmural injury (Roostalu et al., 2018), sug-

gesting but not directly proving a putative contribution of new SMCs from local stem cells. Using genetic lineage tracing, our study provides direct evidence that adventitial PDGFR α ⁺ Sca1⁺ progenitors expand and differentiate into mature SMCs in this scenario. This finally confirms the long-suspected physiological role of adventitial Sca1⁺ cells in regenerating SMCs in some forms of vessel remodeling.

Although our fate mapping study provides evidence of Sca1⁺ VSCs in smooth muscle regeneration, it does not rule out that other stem cell sources may exist for generating new SMCs. Previous studies have reported that Gli1⁺ cells generate SMCs and contribute to neointima formation after wire injury (Kramann et al., 2016). It is possible that *Gli1-CreER*- and *Sca1-CreER*-labeled cells may not be identical in the artery wall. In future studies, it would be interesting to examine whether Gli1⁺Sca1⁻ cells and Gli1⁻Sca1⁺ cells respond differently to wire injury and adopt distinct cell fates. In our study, after more severe transmural injury, Sca1-derived SMCs constituted over 40% of SMCs in some regions of the vessel wall when labeling efficiency was taken into consideration, indicating a critical and important contribution to functional recovery of vessels after injury. Whether other potential Sca1⁻ stem cell populations residing in the adventitial layer may also have contributed to neointimal formation in this context cannot be resolved with our current lineage tracing models. In the future, identification of other stem cells and quantification of their relative contribution to SMCs may further support the stem cell paradigm for vascular repair and regeneration.

Previous lineage tracing studies showed that endothelial cells undergo endothelial-to-mesenchymal transition (EndMT) and contribute to neointimal formation during vein graft remodeling (Cooley et al., 2014). EndMT also contributes to neointimal hyperplasia and induces atherogenic differentiation of endothelial cells by expressing the mesenchymal marker α SMA (Moonen et al., 2015). In addition, endothelial cells give rise to fibroblast-like cells through EndMT in atherosclerotic plaques (Evrard et al., 2016). Mechanistically, reduction of fibroblast growth factor (FGF) signaling and activation of endothelial transforming growth factor β (TGF- β) signaling induced EndMT and led to atherosclerotic disease progression (Chen et al., 2015). Fate mapping of endothelial cells in our study showed no SMC contribution in both wire injury and arterial anastomosis injury. This could be due to the different models we used because previous studies mainly used vein graft and atherosclerosis models for the study of EndMT, which might involve different biomechanical stimuli and a different inflammatory milieu compared with the vascular injury models in our study.

The picture that emerges from the present and previous studies is that Sca1⁺ VSCs, and potentially other adventitial stem cell populations, are a backup system that is activated in situations where proliferation of pre-existing SMCs is

(K) Labeling efficiency of PDGFR β ⁺ cells in *Sca1-CreER;Pdgfrb-LSL-Dre;R26-RSR-tdTomato* and *Sca1-CreER;R26-tdTomato* mice.

(L) Percentage of PDGFR β ⁺ cells expressing tdTomato is shown on the right. Data are mean \pm SEM; n = 5; n.s., non-significant.

(M) Schematic showing the experimental strategy.

(N) H&E staining of vessels, showing the successful anastomosis injury model.

(O) Immunostaining for tdTomato and SMC markers, showing no tdTomato⁺ SMCs in the media.

(P) Cartoon image showing Sca1⁺ cell fate after severe injury.

Scale bars, 100 μ m. Each panel is representative of 5 individual biological samples.

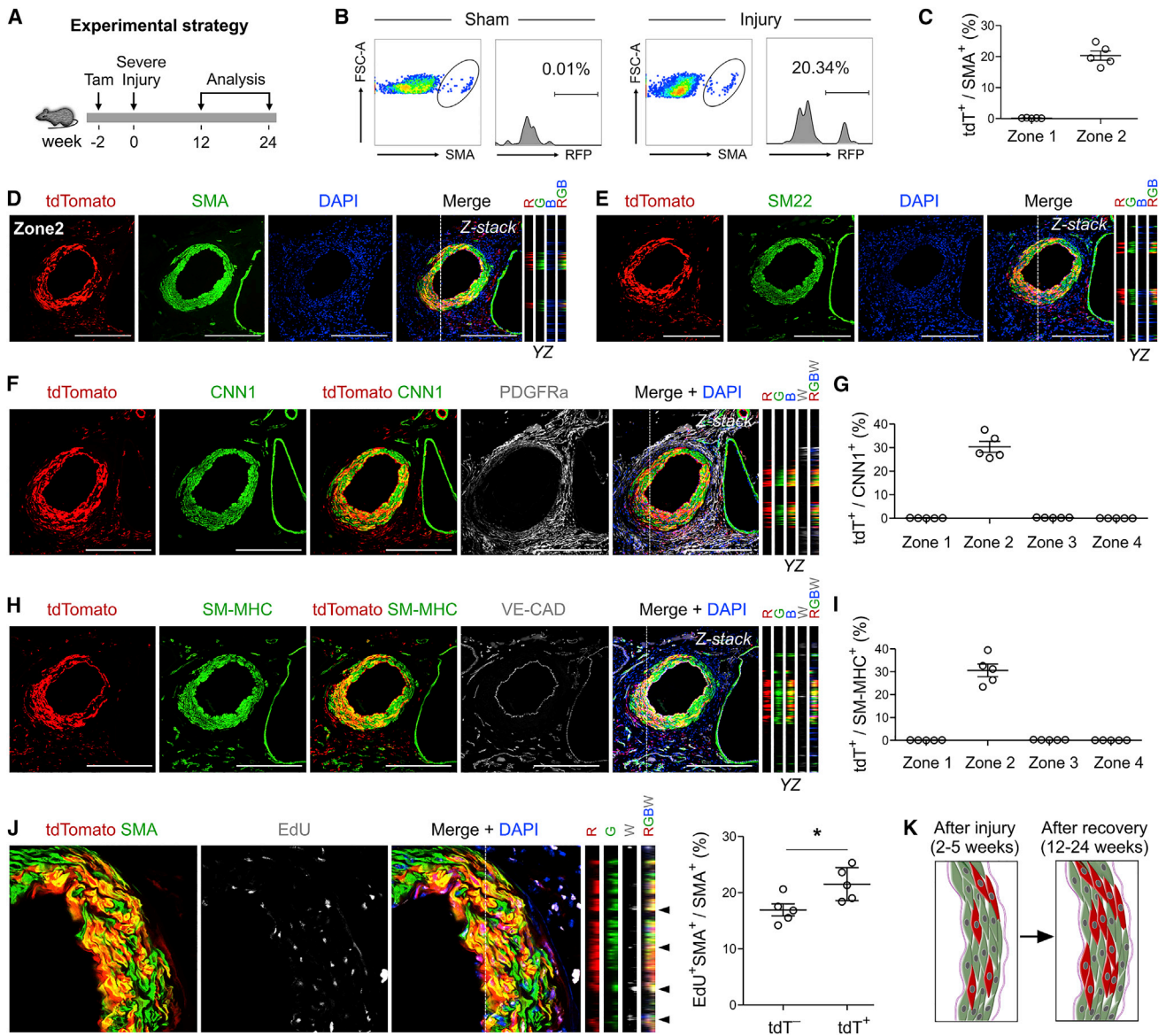


Figure 6. Sca1-Derived SMCs Are More Competent to Expand for Full Recovery

(A) Schematic diagram showing the experimental strategy.

(B) Flow cytometry analysis of Sca1-derived SMCs.

(C) Quantification of the percentage of SMCs derived from Sca1⁺ cells by fluorescence-activated cell sorting (FACS).

(D and E) Immunostaining for tdTomato and SMA (D) and SM22 (E) on tissue sections.

(F) Immunostaining for tdTomato, CNN1, and PDGFRa on tissue sections.

(G) Quantification of the percentage of CNN1⁺ cells expressing tdTomato. Data are mean ± SEM; n = 5.

(H) Immunostaining for tdTomato, SM-MHC, and VE-cadherin (VE-CAD) on tissue sections.

(I) Quantification of the percentage of SM-MHC⁺ cells expressing tdTomato. Data are mean ± SEM; n = 5.

(J) Immunostaining for tdTomato, SMA, and EdU on tissue sections. Arrowheads, EdU⁺SMA⁺tdTomato⁺ cells. Also shown is quantification of the percentage of tdTomato⁻ or tdTomato⁺ SMCs expressing EdU. Data are mean ± SEM; n = 5; *p < 0.05.

(K) Cartoon image showing expansion of tdTomato⁺ SMCs during recovery.

Scale bars, 100 μm. YZ indicates signals from the dotted lines on z stack images in (D)–(F), (H), and (J). RGBW indicates red, green, blue, and white signals in each channel. Each image is representative of 5 individual biological samples.

insufficient. Under homeostasis and after wire injury, pre-existing SMCs are the major source for SMCs, but under conditions where there is significant loss of local SMCs (Roostalu et al., 2018) or local SMC proliferation is impaired (Hu et al.,

2004), stem cells from the adventitia may act as facultative stem cells to migrate into media and differentiate into SMCs for vascular repair and regeneration. Disruption of the elastic lamellae, such as what is seen after transversal sectioning

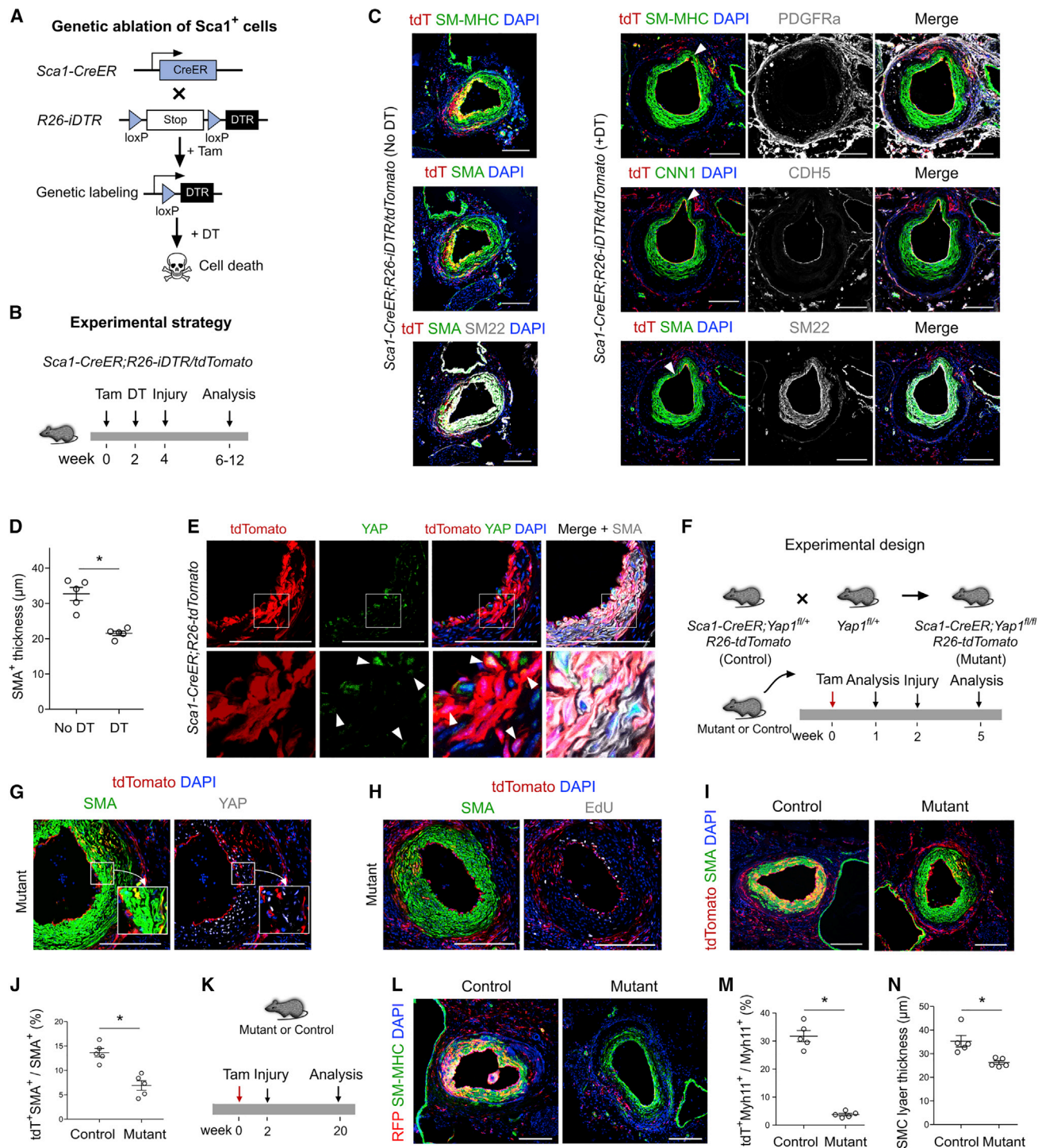


Figure 7. Genetic Ablation of *Sca1*⁺ Cells and *Yap1* Deletion Impaired Vessel Repair and Recovery

(A) Schematic diagram showing genetic ablation of *Sca1*⁺ cells.

(B) Schematic diagram showing the experimental strategy.

(C) Immunostaining for tdTomato, SM-MHC, CNN1, SMA, SM22, PDGFR α , or CDH5 on tissue sections collected 12 weeks after injury. Arrowheads indicate reduced SMCs coverage of the vessel wall.

(D) Quantification of cells expressing SMA.

(E) Immunostaining for tdTomato, SMA, and YAP on *Sca1*-CreER;*R26*-tdTomato sections collected 5 weeks after severe injury. Arrowheads indicate EdU⁺ *Sca1*-derived SMCs in zone 2.

(F) Schematic diagram showing the strategy for *Yap1* deletion (mutant) and the littermate control.

(legend continued on next page)

and anastomosis, could also be an important requirement that facilitates migration of adventitial cells to the media and intima. The adventitial layer of the vessel wall could therefore be viewed as a compartment that provides an appropriate microenvironment for vascular progenitor or stem cells (Zhang et al., 2018) and that may be integral to vascular healing and pathophysiology under some conditions (Psaltis and Simari, 2015). Some of the human vascular pathologies in which such mechanisms are more likely to be involved include transplant vasculopathy, vein graft arteriosclerosis, collateral formation, and arteriogenesis.

This study also shows expansion of Sca1-derived SMCs in vascular recovery after injury. In the future, it would be important to study whether Sca1⁺ VSCs-derived SMCs differ from local SMCs in their propensity to modulate different phenotypes and undergo clonal expansion (Feil et al., 2014; Shankman et al., 2015; Kramann et al., 2016). Equally interesting questions are whether new Sca1⁺ cells derived from differentiated SMCs may have more propensity to re-differentiate into SMCs during neointima formation (Majesky et al., 2017) than other Sca1⁺ populations and whether activation of Sca1 in SMCs during phenotypic switching (Dobnikar et al., 2018) may strengthen their proliferation and function. Altogether, the genetic evidence of Sca1⁺ VSCs for vessel remodeling and repair provides new insights into and raises new questions about the cellular and molecular mechanism for vascular disease and regeneration.

STAR★METHODS

Detailed methods are provided in the online version of this paper and include the following:

- KEY RESOURCES TABLE
- LEAD CONTACT AND MATERIALS AVAILABILITY
- EXPERIMENTAL MODEL AND SUBJECT DETAILS
 - Mice Breeding and Genotyping
 - Femoral Wire Injury
 - Super-microanastomosis model
- METHOD DETAILS
 - Tamoxifen-induced genetic lineage tracing
 - Immunofluorescent Staining and Z stack confocal microscopy
 - Femoral artery cell dissociation
 - Flow cytometry and analysis
 - Single-cell RNA Sequencing preparation and analysis
 - Markov-chain entropy analysis for Sca1⁺PDGFRa⁺ subpopulations
- QUANTIFICATION AND STATISTICAL ANALYSIS
- DATA AND CODE AVAILABILITY

SUPPLEMENTAL INFORMATION

Supplemental Information can be found online at <https://doi.org/10.1016/j.stem.2019.11.010>.

ACKNOWLEDGMENTS

We thank Shanghai Model Organisms Center, Inc. (SMOC) for mouse generation, Dr. Camargo Fernando for Yap-flox mouse, and Baojin Wu, Guoyuan Chen, Zhonghui Weng, and Aimin Huang for animal husbandry. We also thank Wei Bian, Lin Qiu, and members of National Center for Protein Science Shanghai for technical help and assistance with microscopy. This work was supported by the Strategic Priority Research Program of the Chinese Academy of Sciences (CAS; XDA16010507 and XDB19000000), the National Key Research and Development Program of China (2019YFA0110400, 2018YFA0107900, 2018YFA0108100, 2016YFC1300600, and 2017YFC1001303), the Shanghai Zhangjiang Stem Cell Project (ZJ2018-ZD-004), the National Science Foundation of China (31730112, 91639302, 31625019, 91849202, 81761138040, 81872241, 31701292, 31801215, and 31922032), the Youth Innovation Promotion Association of the CAS, the Key Project of Frontier Sciences of the CAS (QYZDB-SSW-SMC003), the Shanghai Science and Technology Commission (19JC1415700, 17ZR1449600, and 17ZR1449800), the Program for Guangdong Introduction Innovative and Entrepreneurial Teams (2017ZT07S347), the Major Program of the Development Fund for the Shanghai Zhangjiang National Innovation Demonstration Zone (Stem Cell Strategic Biobank and Stem Cell Clinical Technology Transformation Platform, ZJ2018-ZD-004), the Shanghai Yangfan Project, the China Postdoctoral Science Foundation, the China Postdoctoral Innovative Talent Support Program, the Young Elite Scientist Sponsorship Program by CAST (2018QNRC001, and 2017QNRC001), Boehringer Ingelheim, a Sanofi-SIBS fellowship, AstraZeneca, and a Royal Society Newton advanced fellowship.

AUTHOR CONTRIBUTIONS

J.T., H.W., X.H., and B.Z. designed the study, performed experiments, and analyzed the data. Huan.Zhu., Y.L., L.H., Hui.Zhang., W.P., K.L., and Huan.Zhao. bred the mice, analyzed the data, and performed experiments. J.F.B., Y.Y., Y.J., Y.N., X.T., and L.Z. provided valuable comments, analyzed the data, and edited the manuscript. F.L. and D.G. performed single-cell RNA sequencing analysis. B.Z. conceived and supervised the study and wrote the manuscript.

DECLARATION OF INTERESTS

The authors declare no competing interests.

Received: May 29, 2019

Revised: September 24, 2019

Accepted: November 18, 2019

Published: December 26, 2019

REFERENCES

- Barrington, K.G., and Matsumura, M.E. (2007). The proteasome inhibitor lactacystin attenuates growth and migration of vascular smooth muscle cells and limits the response to arterial injury. *Exp. Clin. Cardiol.* 12, 119–124.
- Beltrami, A.P., Barlucchi, L., Torella, D., Baker, M., Limana, F., Chimenti, S., Kasahara, H., Rota, M., Musso, E., Urbanek, K., et al. (2003). Adult cardiac

(G and H) Immunostaining for tdTomato, SMA, and YAP (G) and EdU (H) on mutant tissue sections.

(I) Immunostaining for tdTomato and SMA on control or mutant tissue sections.

(J) Quantification of the percentage of SMA⁺ cells expressing tdTomato. Data are mean ± SEM; n = 5; *p < 0.05.

(K) Experimental strategy for the long-term tracing study (20 weeks).

(L) Immunostaining for tdTomato and SM-MHC on control or mutant tissue sections.

(M) Quantification of the percentage of SMMHC⁺ cells expressing tdTomato. Data are mean ± SEM; n = 5; *p < 0.05.

(N) Quantification of the thickness of SMC layers.

Scale bars, 100 μm. Each figure is representative of 5 individual biological samples.

- stem cells are multipotent and support myocardial regeneration. *Cell* 114, 763–776.
- Bennett, M.R., Sinha, S., and Owens, G.K. (2016). Vascular Smooth Muscle Cells in Atherosclerosis. *Circ. Res.* 118, 692–702.
- Bentzon, J.F., and Majesky, M.W. (2018). Lineage tracking of origin and fate of smooth muscle cells in atherosclerosis. *Cardiovasc. Res.* 114, 492–500.
- Bentzon, J.F., Weile, C., Sondergaard, C.S., Hindkjaer, J., Kassem, M., and Falk, E. (2006). Smooth muscle cells in atherosclerosis originate from the local vessel wall and not circulating progenitor cells in ApoE knockout mice. *Arterioscler. Thromb. Vasc. Biol.* 26, 2696–2702.
- Bentzon, J.F., Sondergaard, C.S., Kassem, M., and Falk, E. (2007). Smooth muscle cells healing atherosclerotic plaque disruptions are of local, not blood, origin in apolipoprotein E knockout mice. *Circulation* 116, 2053–2061.
- Buch, T., Heppner, F.L., Tertilt, C., Heinen, T.J., Kremer, M., Wunderlich, F.T., Jung, S., and Waisman, A. (2005). A Cre-inducible diphtheria toxin receptor mediates cell lineage ablation after toxin administration. *Nat. Methods* 2, 419–426.
- Chappell, J., Harman, J.L., Narasimhan, V.M., Yu, H., Foote, K., Simons, B.D., Bennett, M.R., and Jørgensen, H.F. (2016). Extensive Proliferation of a Subset of Differentiated, yet Plastic, Medial Vascular Smooth Muscle Cells Contributes to Neointimal Formation in Mouse Injury and Atherosclerosis Models. *Circ. Res.* 119, 1313–1323.
- Chen, P.Y., Qin, L., Baeyens, N., Li, G., Afolabi, T., Budatha, M., Tellides, G., Schwartz, M.A., and Simons, M. (2015). Endothelial-to-mesenchymal transition drives atherosclerosis progression. *J. Clin. Invest.* 125, 4514–4528.
- Chen, Q., Zhang, H., Liu, Y., Adams, S., Eilken, H., Stehling, M., Corada, M., Dejana, E., Zhou, B., and Adams, R.H. (2016). Endothelial cells are progenitors of cardiac pericytes and vascular smooth muscle cells. *Nat. Commun.* 7, 12422.
- Cherepanova, O.A., Gomez, D., Shankman, L.S., Swiatlowska, P., Williams, J., Sarmiento, O.F., Alencar, G.F., Hess, D.L., Bevard, M.H., Greene, E.S., et al. (2016). Activation of the pluripotency factor OCT4 in smooth muscle cells is atheroprotective. *Nat. Med.* 22, 657–665.
- Cheung, C., Bernardo, A.S., Trotter, M.W., Pedersen, R.A., and Sinha, S. (2012). Generation of human vascular smooth muscle subtypes provides insight into embryological origin-dependent disease susceptibility. *Nat. Biotechnol.* 30, 165–173.
- Cooley, B.C., Nevado, J., Mellad, J., Yang, D., St Hilaire, C., Negro, A., Fang, F., Chen, G., San, H., Walts, A.D., et al. (2014). TGF- β signaling mediates endothelial-to-mesenchymal transition (EndMT) during vein graft remodeling. *Sci. Transl. Med.* 6, 227ra34.
- DeBakey, M.E., Lawrie, G.M., and Glaeser, D.H. (1985). Patterns of atherosclerosis and their surgical significance. *Ann. Surg.* 201, 115–131.
- Dettman, R.W., Denetclaw, W., Jr., Ordahl, C.P., and Bristow, J. (1998). Common epicardial origin of coronary vascular smooth muscle, perivascular fibroblasts, and intermyocardial fibroblasts in the avian heart. *Dev. Biol.* 193, 169–181.
- Dobnikar, L., Taylor, A.L., Chappell, J., Oldach, P., Harman, J.L., Oerton, E., Dzierzak, E., Bennett, M.R., Spivakov, M., and Jørgensen, H.F. (2018). Disease-relevant transcriptional signatures identified in individual smooth muscle cells from healthy mouse vessels. *Nat. Commun.* 9, 4567.
- Evrard, S.M., Lecce, L., Michelis, K.C., Nomura-Kitabayashi, A., Pandey, G., Purushothaman, K.R., d'Escarmad, V., Li, J.R., Hadri, L., Fujitani, K., et al. (2016). Endothelial to mesenchymal transition is common in atherosclerotic lesions and is associated with plaque instability. *Nat. Commun.* 7, 11853.
- Feil, S., Fehrenbacher, B., Lukowski, R., Essmann, F., Schulze-Osthoff, K., Schaller, M., and Feil, R. (2014). Transdifferentiation of vascular smooth muscle cells to macrophage-like cells during atherogenesis. *Circ. Res.* 115, 662–667.
- Gittenberger-de Groot, A.C., Vrancken Peeters, M.P., Mentink, M.M., Gourdie, R.G., and Poelmann, R.E. (1998). Epicardium-derived cells contribute a novel population to the myocardial wall and the atrioventricular cushions. *Circ. Res.* 82, 1043–1052.
- He, W., Barak, Y., Hevener, A., Olson, P., Liao, D., Le, J., Nelson, M., Ong, E., Olefsky, J.M., and Evans, R.M. (2003). Adipose-specific peroxisome proliferator-activated receptor gamma knockout causes insulin resistance in fat and liver but not in muscle. *Proc. Natl. Acad. Sci. USA* 100, 15712–15717.
- He, L., Huang, X., Kanisicak, O., Li, Y., Wang, Y., Li, Y., Pu, W., Liu, Q., Zhang, H., Tian, X., et al. (2017). Preexisting endothelial cells mediate cardiac neovascularization after injury. *J. Clin. Invest.* 127, 2968–2981.
- Hu, Y., Zhang, Z., Torsney, E., Afzal, A.R., Davison, F., Metzler, B., and Xu, Q. (2004). Abundant progenitor cells in the adventitia contribute to atherosclerosis of vein grafts in ApoE-deficient mice. *J. Clin. Invest.* 113, 1258–1265.
- Jacobsen, K., Lund, M.B., Shim, J., Gunnarsen, S., Führtbauer, E.M., Kjolby, M., Carramolino, L., and Bentzon, J.F. (2017). Diverse cellular architecture of atherosclerotic plaque derives from clonal expansion of a few medial SMCs. *JCI Insight* 2, 95890.
- Jiang, X., Rowitch, D.H., Soriano, P., McMahon, A.P., and Sucov, H.M. (2000). Fate of the mammalian cardiac neural crest. *Development* 127, 1607–1616.
- Kajstura, J., Rota, M., Hall, S.R., Hosoda, T., D'Amario, D., Sanada, F., Zheng, H., Ogórek, B., Rondon-Clavo, C., Ferreira-Martins, J., et al. (2018). Retraction. *N. Engl. J. Med.* 379, 1870.
- Kapadia, M.R., Eng, J.W., Jiang, Q., Stoyanovsky, D.A., and Kibbe, M.R. (2009). Nitric oxide regulates the 26S proteasome in vascular smooth muscle cells. *Nitric Oxide* 20, 279–288.
- Kramann, R., Goettsch, C., Wongboonsin, J., Iwata, H., Schneider, R.K., Kuppe, C., Kaesler, N., Chang-Panesso, M., Machado, F.G., Gratwohl, S., et al. (2016). Adventitial MSC-like Cells Are Progenitors of Vascular Smooth Muscle Cells and Drive Vascular Calcification in Chronic Kidney Disease. *Cell Stem Cell* 19, 628–642.
- Kühbandner, S., Brummer, S., Metzger, D., Chambon, P., Hofmann, F., and Feil, R. (2000). Temporally controlled somatic mutagenesis in smooth muscle. *Genesis* 28, 15–22.
- Leroux-Berger, M., Queguiner, I., Maciel, T.T., Ho, A., Relaix, F., and Kempf, H. (2011). Pathologic calcification of adult vascular smooth muscle cells differs on their crest or mesodermal embryonic origin. *J. Bone Miner. Res.* 26, 1543–1553.
- Liu, Q., Huang, X., Zhang, H., Tian, X., He, L., Yang, R., Yan, Y., Wang, Q.D., Gillich, A., and Zhou, B. (2015). c-kit(+) cells adopt vascular endothelial but not epithelial cell fates during lung maintenance and repair. *Nat. Med.* 21, 866–868.
- Liu, Q., Liu, K., Cui, G., Huang, X., Yao, S., Guo, W., Qin, Z., Li, Y., Yang, R., Pu, W., et al. (2019). Lung regeneration by multipotent stem cells residing at the bronchioalveolar-duct junction. *Nat. Genet.* 51, 728–738.
- Madisen, L., Garner, A., Shimaoka, D., Chuong, A., Klapoetke, N., Li, L., van der Bourg, A., Niino, Y., Eglolf, L., Monetti, C., et al. (2015). Transgenic mice for intersectional targeting of neural sensors and effectors with high specificity and performance. *Neuron* 85, 942–958.
- Madisen, L., Zwingman, T.A., Sunkin, S.M., Oh, S.W., Zariwala, H.A., Gu, H., Ng, L.L., Palmiter, R.D., Hawrylycz, M.J., Jones, A.R., et al. (2010). A robust and high-throughput Cre reporting and characterization system for the whole mouse brain. *Nat. Neurosci.* 13, 133–140.
- Majesky, M.W., Dong, X.R., Regan, J.N., and Hoglund, V.J. (2011). Vascular smooth muscle progenitor cells: building and repairing blood vessels. *Circ. Res.* 108, 365–377.
- Majesky, M.W., Horita, H., Ostriker, A., Lu, S., Regan, J.N., Bagchi, A., Dong, X.R., Poczobutt, J., Nemenoff, R.A., and Weiser-Evans, M.C. (2017). Differentiated Smooth Muscle Cells Generate a Subpopulation of Resident Vascular Progenitor Cells in the Adventitia Regulated by Klf4. *Circ. Res.* 120, 296–311.
- Mooney, J.R., Lee, E.S., Schmidt, M., Maleszewska, M., Koerts, J.A., Brouwer, L.A., van Kooten, T.G., van Luyn, M.J., Zeebregts, C.J., Krenning, G., and Harmsen, M.C. (2015). Endothelial-to-mesenchymal transition contributes to fibro-proliferative vascular disease and is modulated by fluid shear stress. *Cardiovasc. Res.* 108, 377–386.

- Naglich, J.G., Metherall, J.E., Russell, D.W., and Eidels, L. (1992). Expression cloning of a diphtheria toxin receptor: identity with a heparin-binding EGF-like growth factor precursor. *Cell* 69, 1051–1061.
- Nemenoff, R.A., Horita, H., Ostriker, A.C., Furgeson, S.B., Simpson, P.A., VanPutten, V., Crossno, J., Offermanns, S., and Weiser-Evans, M.C. (2011). SDF-1 α induction in mature smooth muscle cells by inactivation of PTEN is a critical mediator of exacerbated injury-induced neointima formation. *Arterioscler. Thromb. Vasc. Biol.* 31, 1300–1308.
- Nguyen, A.T., Gomez, D., Bell, R.D., Campbell, J.H., Clowes, A.W., Gabbiani, G., Giachelli, C.M., Parmacek, M.S., Raines, E.W., Rusch, N.J., et al. (2013). Smooth muscle cell plasticity: fact or fiction? *Circ. Res.* 112, 17–22.
- Osman, I., He, X., Liu, J., Dong, K., Wen, T., Zhang, F., Yu, L., Hu, G., Xin, H., Zhang, W., and Zhou, J. (2019). TEAD1 (TEA Domain Transcription Factor 1) Promotes Smooth Muscle Cell Proliferation Through Upregulating SLC1A5 (Solute Carrier Family 1 Member 5)-Mediated Glutamine Uptake. *Circ. Res.* 124, 1309–1322.
- Passman, J.N., Dong, X.R., Wu, S.P., Maguire, C.T., Hogan, K.A., Bautch, V.L., and Majesky, M.W. (2008). A sonic hedgehog signaling domain in the arterial adventitia supports resident Sca1+ smooth muscle progenitor cells. *Proc. Natl. Acad. Sci. USA* 105, 9349–9354.
- Pérez-Pomares, J.M., Macías, D., García-Garrido, L., and Muñoz-Chápuli, R. (1998). The origin of the subepicardial mesenchyme in the avian embryo: an immunohistochemical and quail-chick chimera study. *Dev. Biol.* 200, 57–68.
- Perlman, H., Maillard, L., Krasinski, K., and Walsh, K. (1997). Evidence for the rapid onset of apoptosis in medial smooth muscle cells after balloon injury. *Circulation* 95, 981–987.
- Psaltis, P.J., and Simari, R.D. (2015). Vascular wall progenitor cells in health and disease. *Circ. Res.* 116, 1392–1412.
- Pu, W., He, L., Han, X., Tian, X., Li, Y., Zhang, H., Liu, Q., Huang, X., Zhang, L., Wang, Q.D., et al. (2018). Genetic Targeting of Organ-Specific Blood Vessels. *Circ. Res.* 123, 86–99.
- Ramalho-Santos, M., Yoon, S., Matsuzaki, Y., Mulligan, R.C., and Melton, D.A. (2002). “Stemness”: transcriptional profiling of embryonic and adult stem cells. *Science* 298, 597–600.
- Roostalu, U., Aldeiri, B., Albertini, A., Humphreys, N., Simonsen-Jackson, M., Wong, J.K.F., and Cossu, G. (2018). Distinct Cellular Mechanisms Underlie Smooth Muscle Turnover in Vascular Development and Repair. *Circ. Res.* 122, 267–281.
- Ruddy, J.M., Jones, J.A., Spinale, F.G., and Ikonomidis, J.S. (2008). Regional heterogeneity within the aorta: relevance to aneurysm disease. *J. Thorac. Cardiovasc. Surg.* 136, 1123–1130.
- Sainz, J., Al Haj Zen, A., Caligiuri, G., Demerens, C., Urbain, D., Lemitre, M., and Lafont, A. (2006). Isolation of “side population” progenitor cells from healthy arteries of adult mice. *Arterioscler. Thromb. Vasc. Biol.* 26, 281–286.
- Saiura, A., Sata, M., Hirata, Y., Nagai, R., and Makuuchi, M. (2001). Circulating smooth muscle progenitor cells contribute to atherosclerosis. *Nat. Med.* 7, 382–383.
- Sata, M., Saiura, A., Kunisato, A., Tojo, A., Okada, S., Tokuhisa, T., Hirai, H., Makuuchi, M., Hirata, Y., and Nagai, R. (2002). Hematopoietic stem cells differentiate into vascular cells that participate in the pathogenesis of atherosclerosis. *Nat. Med.* 8, 403–409.
- Sawada, H., Rateri, D.L., Moorleghen, J.J., Majesky, M.W., and Daugherty, A. (2017). Smooth Muscle Cells Derived From Second Heart Field and Cardiac Neural Crest Reside in Spatially Distinct Domains in the Media of the Ascending Aorta—Brief Report. *Arterioscler. Thromb. Vasc. Biol.* 37, 1722–1726.
- Schlegelmilch, K., Mohseni, M., Kirak, O., Pruszk, J., Rodriguez, J.R., Zhou, D., Kreger, B.T., Vasioukhin, V., Avruch, J., Brummelkamp, T.R., and Camargo, F.D. (2011). Yap1 acts downstream of α -catenin to control epidermal proliferation. *Cell* 144, 782–795.
- Shankman, L.S., Gomez, D., Cherepanova, O.A., Salmon, M., Alencar, G.F., Haskins, R.M., Swiatlowska, P., Newman, A.A., Greene, E.S., Straub, A.C., et al. (2015). KLF4-dependent phenotypic modulation of smooth muscle cells has a key role in atherosclerotic plaque pathogenesis. *Nat. Med.* 21, 628–637.
- Shi, J., Teschendorff, A.E., Chen, W., Chen, L., and Li, T. (2018). Quantifying Waddington’s epigenetic landscape: a comparison of single-cell potency measures. *Brief. Bioinform.*, bby019.
- Subramanian, A., Tamayo, P., Mootha, V.K., Mukherjee, S., Ebert, B.L., Gillette, M.A., Paulovich, A., Pomeroy, S.L., Golub, T.R., Lander, E.S., and Mesirov, J.P. (2005). Gene set enrichment analysis: a knowledge-based approach for interpreting genome-wide expression profiles. *Proc. Natl. Acad. Sci. USA* 102, 15545–15550.
- Takayama, T., Shi, X., Wang, B., Franco, S., Zhou, Y., DiRenzo, D., Kent, A., Hartig, P., Zent, J., and Guo, L.W. (2015). A murine model of arterial restenosis: technical aspects of femoral wire injury. *J. Vis. Exp.* (97).
- Tang, Z., Wang, A., Yuan, F., Yan, Z., Liu, B., Chu, J.S., Helms, J.A., and Li, S. (2012). Differentiation of multipotent vascular stem cells contributes to vascular diseases. *Nat. Commun.* 3, 875.
- Tang, Z., Wang, A., Wang, D., and Li, S. (2013). Smooth muscle cells: to be or not to be? Response to Nguyen et al. *Circ. Res.* 112, 23–26.
- Teschendorff, A.E., and Enver, T. (2017). Single-cell entropy for accurate estimation of differentiation potency from a cell’s transcriptome. *Nat. Commun.* 8, 15599.
- Tsai, T.N., Kirton, J.P., Campagnolo, P., Zhang, L., Xiao, Q., Zhang, Z., Wang, W., Hu, Y., and Xu, Q. (2012). Contribution of stem cells to neointimal formation of decellularized vessel grafts in a novel mouse model. *Am. J. Pathol.* 181, 362–373.
- van Berlo, J.H., Kanisicak, O., Maillet, M., Vagnozzi, R.J., Karch, J., Lin, S.C., Middleton, R.C., Marbán, E., and Molkenkin, J.D. (2014). c-kit+ cells minimally contribute cardiomyocytes to the heart. *Nature* 509, 337–341.
- Van Keymeulen, A., Rocha, A.S., Ousset, M., Beck, B., Bouvencourt, G., Rock, J., Sharma, N., Dekoninck, S., and Blanpain, C. (2011). Distinct stem cells contribute to mammary gland development and maintenance. *Nature* 479, 189–193.
- Waldo, K.L., Hutson, M.R., Stadt, H.A., Zdanowicz, M., Zdanowicz, J., and Kirby, M.L. (2005). Cardiac neural crest is necessary for normal addition of the myocardium to the arterial pole from the secondary heart field. *Dev. Biol.* 281, 66–77.
- Wang, Y., Nakayama, M., Pitulescu, M.E., Schmidt, T.S., Bochenek, M.L., Sakakibara, A., Adams, S., Davy, A., Deutsch, U., Lüthi, U., et al. (2010). Ephrin-B2 controls VEGF-induced angiogenesis and lymphangiogenesis. *Nature* 465, 483–486.
- Wang, Y., Hu, G., Liu, F., Wang, X., Wu, M., Schwarz, J.J., and Zhou, J. (2014). Deletion of yes-associated protein (YAP) specifically in cardiac and vascular smooth muscle cells reveals a crucial role for YAP in mouse cardiovascular development. *Circ. Res.* 114, 957–965.
- Wasteson, P., Johansson, B.R., Jukkola, T., Breuer, S., Akyürek, L.M., Partanen, J., and Lindahl, P. (2008). Developmental origin of smooth muscle cells in the descending aorta in mice. *Development* 135, 1823–1832.
- Yeligar, S.M., Kang, B.Y., Bijli, K.M., Kleinhenz, J.M., Murphy, T.C., Torres, G., San Martin, A., Suttiff, R.L., and Hart, C.M. (2018). PPAR γ Regulates Mitochondrial Structure and Function and Human Pulmonary Artery Smooth Muscle Cell Proliferation. *Am. J. Respir. Cell Mol. Biol.* 58, 648–657.
- Zhang, L., and Xu, Q. (2017). Vascular Progenitors and Smooth Muscle Cells: Chicken and Egg? *Circ. Res.* 120, 246–248.
- Zhang, H., Pu, W., Li, G., Huang, X., He, L., Tian, X., Liu, Q., Zhang, L., Wu, S.M., Sucov, H.M., and Zhou, B. (2016a). Endocardium Minimally Contributes to Coronary Endothelium in the Embryonic Ventricular Free Walls. *Circ. Res.* 118, 1880–1893.
- Zhang, H., Pu, W., Tian, X., Huang, X., He, L., Liu, Q., Li, Y., Zhang, L., He, L., Liu, K., et al. (2016b). Genetic lineage tracing identifies endocardial origin of liver vasculature. *Nat. Genet.* 48, 537–543.
- Zhang, L., Issa Bhaloo, S., Chen, T., Zhou, B., and Xu, Q. (2018). Role of Resident Stem Cells in Vessel Formation and Arteriosclerosis. *Circ. Res.* 122, 1608–1624.

STAR★METHODS

KEY RESOURCES TABLE

REAGENT or RESOURCE	SOURCE	IDENTIFIER
Antibodies		
tdTomato	ChromoTek	Cat# ABIN334653; RRID:AB_2209751
VE-CAD	R&D	Cat# AF1002; RRID:AB_2077789
SMA-FITC	Sigma-Aidrich	Cat# F3777; RRID:AB_476977
SM-MHC	Abcam	Cat# AB53219; RRID:AB_2147146
Calponin	Abcam	Cat# AB46794; RRID:AB_2291941
SM22 alpha	Abcam	Cat# AB14106; RRID:AB_443021
PDGFRa	R&D	Cat# AF1062; RRID:AB_2236897
PDGFRb	eBioscience	Cat# 14-1402-82; RRID:AB_467493
Perilipin A	Abcam	Cat# AB61682; RRID:AB_944751
Sca1	Abcam	Cat# AB25031; RRID:AB_448550
YAP	ABclonal	Cat# A1002; RRID:AB_2757539
APC-CD31	eBioscience	Cat# 17-0311-82; RRID:AB_657735
Biotin-Sca-1	BD pharmingen	Cat# 553334; RRID:AB_394790
APC-PDGFRa	eBioscience	Cat# 17-1401-81; RRID:AB_529482
APC-PDGFRb	eBioscience	Cat# 14-1402-82; RRID:AB_467493
Chemicals, Peptides, and Recombinant Proteins		
Tamoxifen	Sigma-Aidrich	T5648
Sucrose	Sigma-Aidrich	S0389
O.C.T.	Tissue-Tek	4583
Donkey serum	JIR	017-000-001
Triton X-100	Sigma-Aidrich	Sigma-X-100
Collagenase I	GIBCO	17018029
PBS	GIBCO	C10010500BT)
DMEM	Hyclone	SH30022.01
Isoflurane gas	Jinan Shengqi Pharm. Co, Ltd.	26675-46-7
Critical Commercial Assays		
Tyramide signal amplification kit	PerkinElmer	NEL749B001KT
Chromium Single Cell 3' Library & Gel Bead Kit v2	10X Genomics	Cat# 120237
Deposited Data		
Single Cell RNA Sequencing	This paper	Seq GEO number: GSE139827
Experimental Models: Organisms/Strains		
Mouse: <i>Sca1-CreER</i>	This paper	Shanghai Biomodel Organism Co., Ltd
Mouse: <i>CD45-Dre</i>	This paper	Shanghai Biomodel Organism Co., Ltd
Mouse: <i>Pdgfrb-LSL-Dre</i>	This paper	Shanghai Biomodel Organism Co., Ltd
Mouse: <i>R26-tdTomato</i>	Madisen et al., 2010	N/A
Mouse: <i>R26-RSR-tdTomato</i>	Zhang et al., 2016a	N/A
Mouse: <i>R26-RSR-LSL-tdTomato</i>	Madisen et al., 2015	N/A
Mouse: <i>Sm22-CreER</i>	Kühbandner et al., 2000	N/A
Mouse: <i>Cdh5-CreER</i>	Wang et al., 2010	N/A
Mouse: <i>Fabp4-Cre</i>	He et al., 2017	N/A
Mouse: <i>PDGFRa-DreER</i>	He et al., 2017	N/A
Mouse: <i>R26-iDTR</i>	Buch et al., 2005	N/A
Mouse: <i>Yap-flox</i>	Schlegelmilch et al., 2011	N/A

(Continued on next page)

Continued

REAGENT or RESOURCE	SOURCE	IDENTIFIER
Software and Algorithms		
GraphPad Prism 6 software	GraphPad Software, Inc.	N/A
FlowJo software	Tree Star, Ashland, Ore	N/A
PhotoLine	https://www.pl32.com/	N/A
Cell Ranger (v.2.1.1)	10X Genomics	https://support.10xgenomics.com
Seurat v2.3	R. Satija Lab	https://satijalab.org/seurat/
R version 3.6.1	The Comprehensive R Archive Network	http://cran.r-project.org/
GSEA version 3.0	Subramanian et al., 2005	http://software.broadinstitute.org/gsea/index.jsp
Cell Ranger (v.2.1.1)	10X Genomics	https://support.10xgenomics.com

LEAD CONTACT AND MATERIALS AVAILABILITY

Requests for further information, reagent, and resource sharing maybe directed to, and will be fulfilled by, the Lead Contact, Bin Zhou (zhoubin@sibs.ac.cn). This study did not generate new unique reagents. Mouse lines reported in this study have been deposited in Shanghai Biomodel Company. The materials, reagents, mice lines, and original data could also be provided on reasonable request.

EXPERIMENTAL MODEL AND SUBJECT DETAILS**Mice Breeding and Genotyping**

All mice studies were proceeding in accordance with the guidelines of the Institutional Animal Care and Use Committee (IACUC) at the Institute for Nutritional Sciences, and the institute of Biochemistry and Cell Biology, Shanghai Institutes for Biological Sciences, Chinese Academy of Science. Mice were bred with normal diet and maintained on a C57BL6/ICR background. *Sca1-CreER*, *CD45-Dre* and *Pdgfrb-LSL-Dre* mice were generated by CRISPR/Cas9 or conventional embryonic stem cell gene targeting methods. Briefly, the cDNA encoding P2A peptide and Cre recombinase fused with a mutant form of the estrogen receptor hormone-binding domain (CreER^{T2}) fusion protein were inserted into the between last exon and 3' UTR of *Sca1* gene. While the cDNA encoding Dre fusion protein were inserted into the CD45 gene locus replacing the endogenous translational start codon ATG, followed by Woodchuck post-transcriptional regulatory element (WPRE) and polyA sequence. *Pdgfrb-LSL-Dre* mice were generated by insertion of Loxp-Stop-Loxp-Dre-WPRE-polyA-Frt-PGK-Neo-Frt into the translational start codon ATG lucs of *Pdgfrb* gene by homologous recombination. The DNA encoding LSL-Dre cassette was then linearized and electroporated into mouse embryonic stem cells. Positive and negative selections of correct targeted ES cell clones were performed by long PCR spanning 5' or 3' homologous arm. Corrected ES cells were injected into blastocyst for generation of chimera. After germline transmission, mice with corrected targeted allele were bred under C57BL6/ICR mixed background. All these mice were generated by Shanghai Biomodel Organism Co., Ltd. Other mouse lines *R26-tdTomato*, *R26-RSR-tdTomato*, *R26-RSR-LSL-tdTomato*, *Sm22-CreER*, *Cdh5-CreER*, *Fabp4-Cre*, *PDGFRa-DreER*, *R26-iDTR*, *Yap-flox* mouse line were reported previously (Buch et al., 2005; He et al., 2003, 2017; Kühbandner et al., 2000; Madisen et al., 2010, 2015; Schlegelmilch et al., 2011; Wang et al., 2010; Zhang et al., 2016). *Sm22-CreER;R26-tdTomato*, *Cdh5-CreER;R26-tdTomato*, *Fabp4-Cre;R26-tdTomato*, *Sca1-CreER;R26-tdTomato* were obtained by crossing with *R26-tdTomato* mice. By crossing *CD45-Dre* with *R26-RSR-tdTomato*, we got *CD45-Dre;R26-RSR-tdTomato* mice. While *Sca1-CreER;PDGFRa-DreER;R26-RSR-LSL-tdTomato* were obtained by *Sca1-CreER* crossing with *PDGFRa-DreER;R26-LSL-RSR-tdTomato* mouse. Furthermore, *Sca1-CreER;R26-tdTomato* crossed with *R26-iDTR* and *Yap^{flox/flox}* to obtain *Sca1-CreER;R26-tdTomato;R26-iDTR* and *Sca1-CreER;R26-tdTomato;Yap^{flox/flox}* mice. The littermates were also used for control experiments. Genomic DNA for genotyping was prepared from mice tail and papered for genotyping by Proteinase K lysed, isopropanol precipitated and 70% ethanol washed. The number of animals be used were approved based on the experiments effects size. All male and female mice were included in the study, and the start point (0 week) for each experiment involves adult mice of 8 weeks old.

Femoral Wire Injury

Femoral artery was performed as described (Takayama et al., 2015). *Sca1-CreER;R26-tdTomato* mice were anesthetized with 2% isoflurane gas using an induction chamber and the core temperature of the animal was maintained by placement upon a 37°C water-heated pad. The breath of mice was controlled at about 120 ~140 breaths per minute and the respiratory volume to 0.3-0.5 mL. The vein and connective tissues around the artery were carefully removed with microsurgery forceps and the femoral artery was isolated. And the end-blunted 31-gauge needle (0.26mm in diameter) was inserted into the isolated femoral artery, then pushed forward for ~5-10 mm toward the iliac artery and left in place for 3 min. The blood flow was reconstituted after ligation of the profunda femoris branch. After 4 weeks for injury, mice were perfused with 4% PFA via the left ventricle for 10 min, and femoral artery were harvested for analysis.

Super-microanastomosis model

Femoral artery super-microanastomosis model was performed in adult mice as described previously (Roostalu et al., 2018). Mice femoral artery was exposed and a suitable nylon monofilament was selected for the IVaS. As the end of a nylon must be smooth to avoid damage to the vessel lumen, we used a razor or surgical knife to produce a clean cut instead of using scissors. Next, the nylon stent was inserted into the vessels, and the vessels were pulled closely together for anastomosis. The vessel wall was carefully sutured using 11-0 nylon. The last one or two stitches were left untied to allow removal of the nylon stent. The IVaS was then removed from the space between the free vessel ends. After reconfirming that the IVaS had securely removed from the vessel, the last one or two stitches were sutured. Finally, the clips were removed and blood flow was restarted. After 2 or 5 weeks injury, mice were perfused with 4% PFA via the left ventricle for 10 min, and femoral artery were harvested for analysis.

METHOD DETAILS

Tamoxifen-induced genetic lineage tracing

For treatment, tamoxifen dissolved in corn oil (20 mg/ml) was introduced by gavage at the indicated time (0.1-0.2 mg/g mouse body weight). For *Sca1-CreER* mice characterization and longtime tracing, mice were treated with tamoxifen twice and then samples were collected in indicated time. For injury models, the mice were subjected to femoral artery injury models at two weeks following cessation of tamoxifen. At the indicated time, mice were sacrificed by CO₂ asphyxiation and femoral arteries were collected for further experiments.

Immunofluorescent Staining and Z stack confocal microscopy

We performed immunostaining as previous reported (Zhang et al., 2016b). Briefly, femoral artery harvested from transgenic mice were wash in PBS for three times, then fixed in 4% PFA for 1 hours. After another washing in PBS for three times, femoral artery with fluorescence reporters were put on agar for the photographed using the Zeiss first (Zeiss AXIO Zoom. V16). Then the collected femoral artery samples were incubated in 30% sucrose until they were fully penetrated and then they were embedded in optimum cutting temperature (O.C.T., Sakura). For each block, 10 μ m thickness cryosections was collected for further immunostaining. Cryosections were air-dried for about 1 hours at room temperature, following by incubation with blocking buffer (5% donkey serum, 0.1% Triton X-100 in PBS) for 30 minutes at room temperature and then incubated with primary antibody overnight at 4°C. In this study, primary antibodies were used as listed: tdTomato or RFP (ChromoTek, ABIN334653, 1:1000), VE-CAD or CDH5 (R&D, AF1002, 1:200), SMA-FITC (Sigma, F3777, 1:500), SM-MHC (Abcam, ab53219, 1:300), Calponin (Abcam, ab46794, 1:300), SM22 alpha (Abcam, ab14106, 1:500), PDGFRa (R&D, AF1062, 1:500), PDGFRb (eBioscience, 14-1402-82, 1:500), Perilipin A (Abcam, ab61682, 1:200), Sca1 (Abcam, ab25031, 1:200), YAP (ABclonal, A1002, 1:500). Signals were detected by using Alexa fluorescence-conjugated secondary antibodies (Invitrogen) for 30 min at room temperature. While for SM-MHC and Calponin staining, HRP or biotin-conjugated secondary antibodies and a tyramide signal amplification kit (PerkinElmer) were used to develop signals. Images were captured Zeiss (LSM 710) laser-scanning confocal microscope from each heart. For Z stack images, 4-8 consecutive XY images were obtained on the Z axis by Zeiss confocal microscope (LSM 710). ImageJ software was used to analyze the collected images. For details, images were merged using the Image color-merge channels function, and Z-projects and color-merge channels function was used to merge images. In the stack, we use an orthogonal view to obtain the signals on the XZ or YZ axis. Merged signals and split channels were used to delineate the signals at single-cell resolution, as described previously.

Femoral artery cell dissociation

To generate single-cell suspensions, femoral arteries isolated from both male and female mice (8 weeks old) were further digested in collagenase I for 30-60 min as described. In detail, femoral arteries were cut into 1mm small pieces, and these small pieces were digested by 1.5 mg/ml collagenase (GIBCO, 17018029) at 37°C, during this process, artery pieces was frequent stirred to ensure full digestion. After sufficient digestion, cells were filtered through a 40- μ m cell strainer, and the collected cells were centrifuged 5 min at 600 g speed. Subsequently, cell pellet was suspended in PBS or DEME for further experiments.

Flow cytometry and analysis

Cells collected from mice femoral artery were stained with fluorochrome-conjugated antibodies, according to the manufacturer's instruction. Isolated cells were stained with APC-CD31 (17-0311-82, eBioscience, 1:200), Biotin-Sca-1 (553334, BD pharmingen, 1:200), APC-PDGFRa (17-1401, eBioscience, 1:200), APC-PDGFRb (14-1402-82, eBioscience, 1:200), FITC-SMA (F3777, sigma, 1:50) for 30 min. For Biotin-Sca-1 staining, streptavidin-APC was incubated for 30 minutes and used to develop signals. Fluorescence labeled cells analyzed was performed using a BD FACS Aria flow cytometry system (BD Biosciences, San Jose, CA), and data were analyzed with FlowJo software (Tree Star, Ashland, Ore) according to protocols described previous.

Single-cell RNA Sequencing preparation and analysis

Single cell library was generated using Chromium Single Cell 3' Library Kit v2. Sequencing of library was performed on Illumina Nova-seq6000 PE150 platform. Aligned reads and gene-barcode matrices were then generated from FASTQ files including Read 1, Read 2 and i7 index using Cell Ranger (v.2.1.1) processing pipeline. Further analysis and visualization were performed with R package Seurat. Threshold of unique counts over 3500 or less than 200 was set to filter cell doublets. Low-quality cells that have > 6%

mitochondrial counts were filtered. 'LogNormalize' method was conducted for normalization for each cell based on the total expression. 'FindVariableGenes' was performed to detect variable genes across the single cells. The key parameters of 'FindClusters' were set with $\text{dims.use} = 1:20$ and $\text{resolution} = 0.2$. The top 10 markers (or all markers if less than 10) were used to plot expression heatmap of marker genes. Pathway enrichment analysis was performed using Metascape (<http://metascape.org/gp/index.html>). Normalized expression value of *Pdgfra* and *Pdgfrb* was used to distinguish fibroblasts and pericytes. In detail, *Pdgfra*⁺ cells were defined with the expression value of *Pdgfra* > 0 and *Pdgfrb* = 0, *Pdgfrb*⁺ cells were defined using the same standard, and cells that have the expression value of *Pdgfra* > 0 and *Pdgfrb* > 0 were clustered into *Pdgfra*⁺/*Pdgfrb*⁺ cells (double positive cells). GSEAI (Gene Set Enrichment Analysis) was performed to determine statistically significant biological pathway based on the normalized expression value according to the software instructions (Subramanian et al., 2005).

Markov-chain entropy analysis for *Sca1*⁺*PDGFRa*⁺ subpopulations

To assess the differentiation potency of the four *Sca1*⁺*PDGFRa*⁺ sub clusters, Markov-chain entropy (MCE) values (Shi et al., 2018) were computed based on normalized expression matrix and protein-protein interaction network. First, normalized expression matrix of these *Sca1*⁺*PDGFRa*⁺ cells was generated with R package Seurat, of which gene symbols were further converted to human Entrez gene IDs with bioDBnet (<https://biodbnet-abcc.ncifcrf.gov/db/db2db.php>). We next constructed the protein-protein interaction network on the basis of the published database (Teschendorff and Enver, 2017). Finally, the MCE values of the four sub clusters were computed. Hypothesis test was performed using the one-way ANOVA.

QUANTIFICATION AND STATISTICAL ANALYSIS

All data were determined from multiple individual biological samples, and presented as mean values \pm standard error of the mean (SEM). The "n" in the study represented the number of biological replicates and was indicated in the manuscript. All mice were randomly assigned to groups (including both male and female), and the investigators who analyzed the samples were blinded to the group allocations. Sample size estimates were not performed. For statistical comparisons, an unpaired two-sided Student's t test was performed using Graphpad Prism software for comparing differences between two groups, and ANOVA test for over two groups. Significance was accepted when $p < 0.05$. All mice were randomly assigned to different experimental groups.

DATA AND CODE AVAILABILITY

The accession number for the Single cell RNA sequencing data for mouse femoral artery reported in this paper is GSE139827.

Cell Stem Cell, Volume 26

Supplemental Information

Arterial Sca1⁺ Vascular Stem Cells Generate

***De Novo* Smooth Muscle for Artery Repair**

and Regeneration

Juan Tang, Haixiao Wang, Xiuzhen Huang, Fei Li, Huan Zhu, Yan Li, Lingjuan He, Hui Zhang, Wenjuan Pu, Kuo Liu, Huan Zhao, Jacob Fog Bentzon, Ying Yu, Yong Ji, Yu Nie, Xueying Tian, Li Zhang, Dong Gao, and Bin Zhou

A

Cluster	nCells	Percentage(%)
1 Fibr_Per1_1	1191	22.25
2 Fibr_Per1_2	1508	28.17
3 Fibr_Per1_3	181	3.38
4 Fibr_Per1_4	129	2.41
5 Endothelial_1	274	5.12
6 Endothelial_2	79	1.48
7 T_cell	189	3.53
8 B_cell	405	7.57
9 Macrophage	907	16.94
10 Monocytes	437	8.16
11 Neutrophil	53	0.99

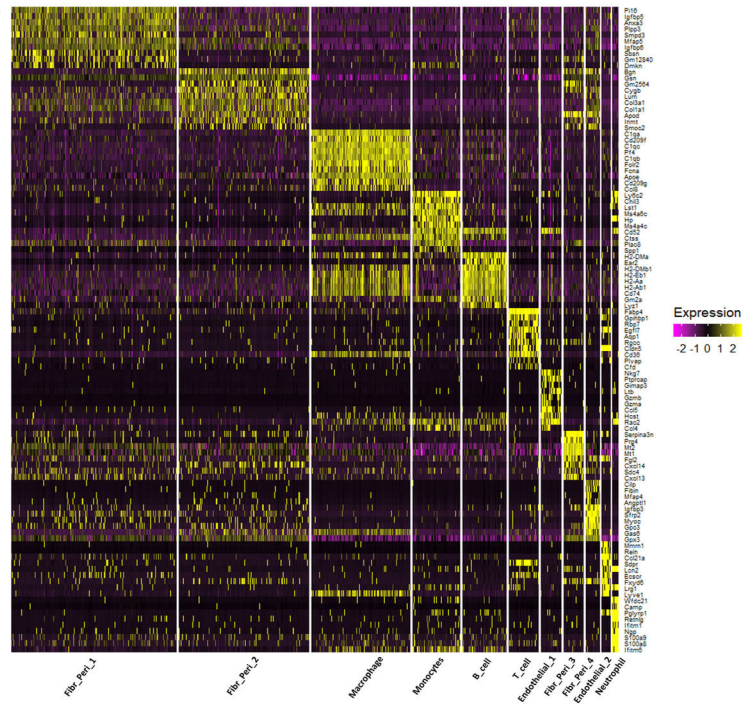
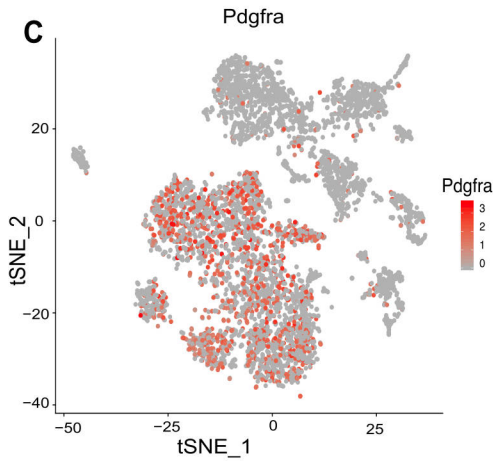
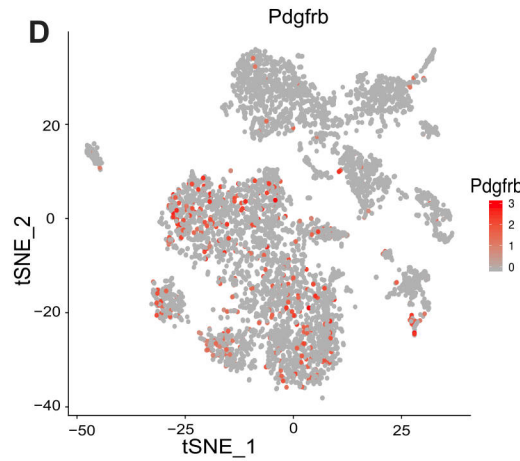
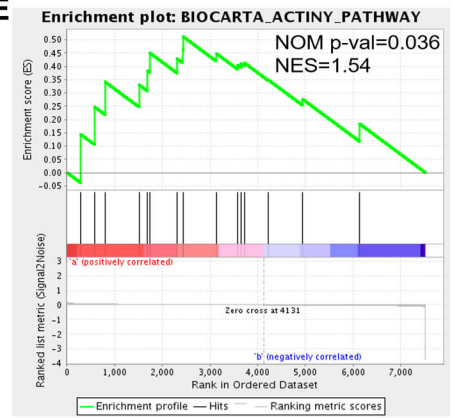
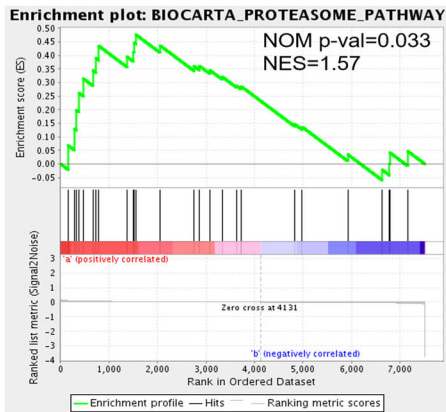
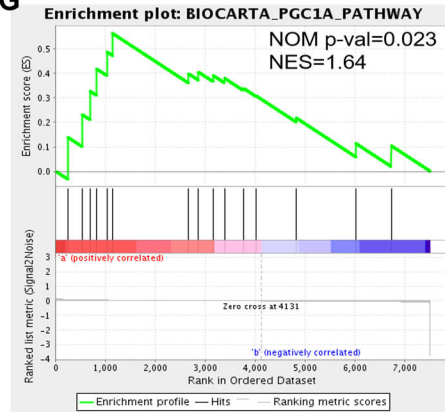
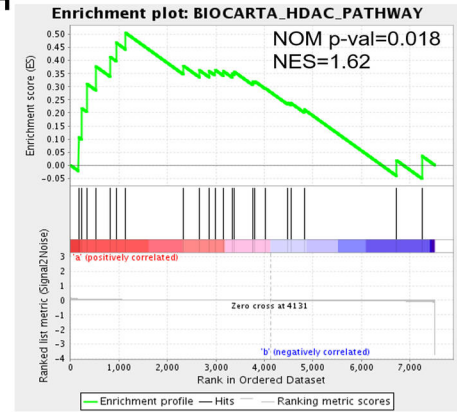
B**C****D****E****F****G****H**

Figure S1 (Related to Figure 1) . Single-cell RNA sequencing analysis of femoral artery cell distribution. (A) Each cell clustering number and percentage in t-distributed stochastic neighbor embedding (t-SNE) plot of 5353 cells isolated from femoral arteries. **(B)** Heat map of gene expression of the 11 cell clusters. **(C,D)** Distribution of PDGFRa and PDGFRb expression across all subpopulations of femoral artery cells. **(E-H)** Signaling pathways significantly enriched in PDGFRa⁺ cells using BioCarta gene sets for GSEA ($P < 0.05$).

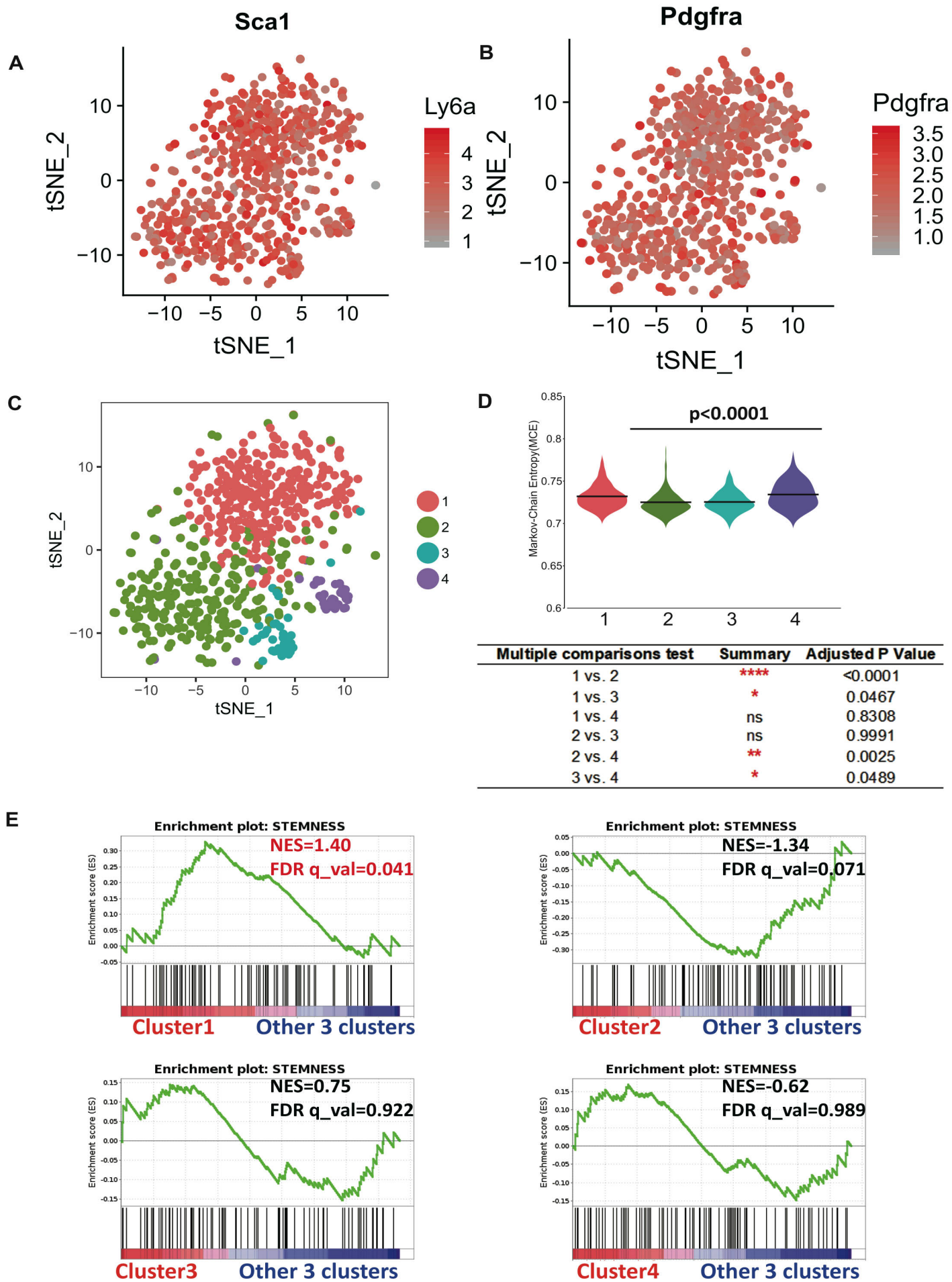


Figure S2 (Related to Figure 1). Single-cell RNA sequencing analysis of Sca1+PDGFRa+ cells from femoral artery. (A-B) Gene expression levels of Sca1/Ly6a (A) or Pdgfra (B) in t-SNE map of Sca1+PDGFRa+ cells. **(C)** Visualization of unsupervised clustering in t-SNE plot of Sca1+PDGFRa+ cells. **(D)** Violin plot of Markov-Chain Entropy (MCE) values in the four clusters (top panel) and table for multiple comparison test (bottom panel). **(E)** Enrichment plot of GSEA for every cluster versus the other 3 clusters using stemness genes.

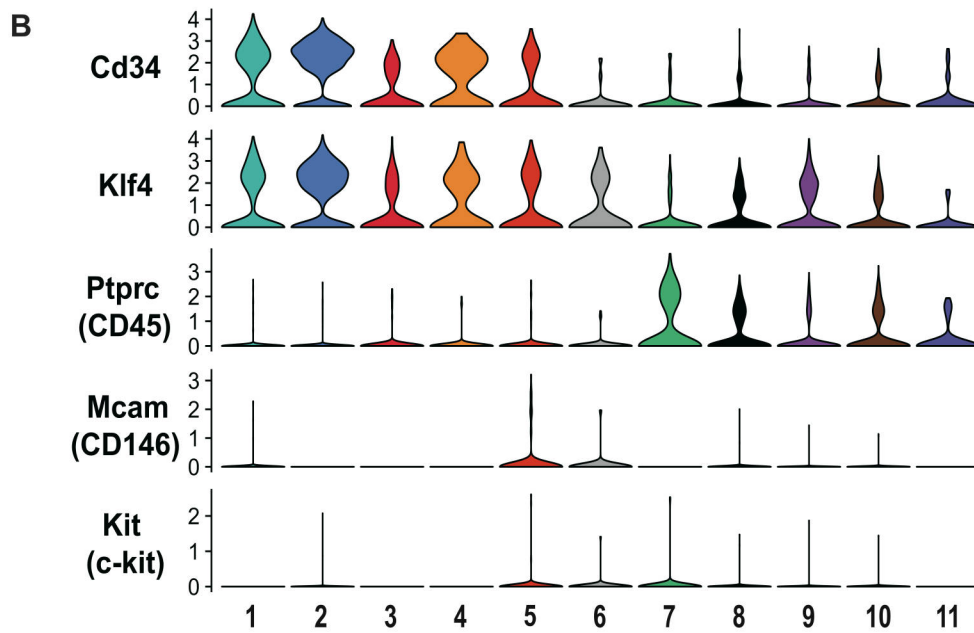
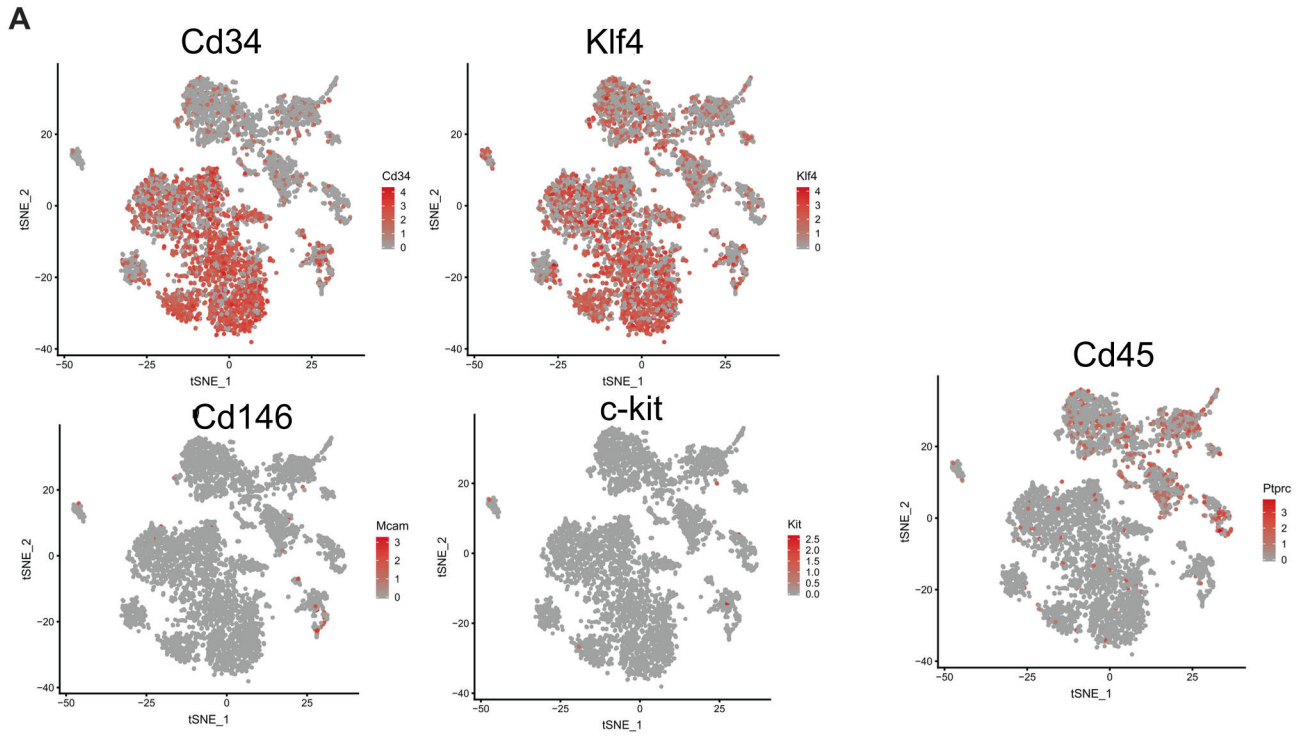


Figure S3 (Related to Figure 1). Single-cell RNA sequencing analysis of adventitial progenitor gene expression in femoral artery cells. (A) Distribution of gene for adventitial progenitor cells across all the subpopulations. **(B)** Violin plots showing the expression levels of relative genes across the 11 clusters.

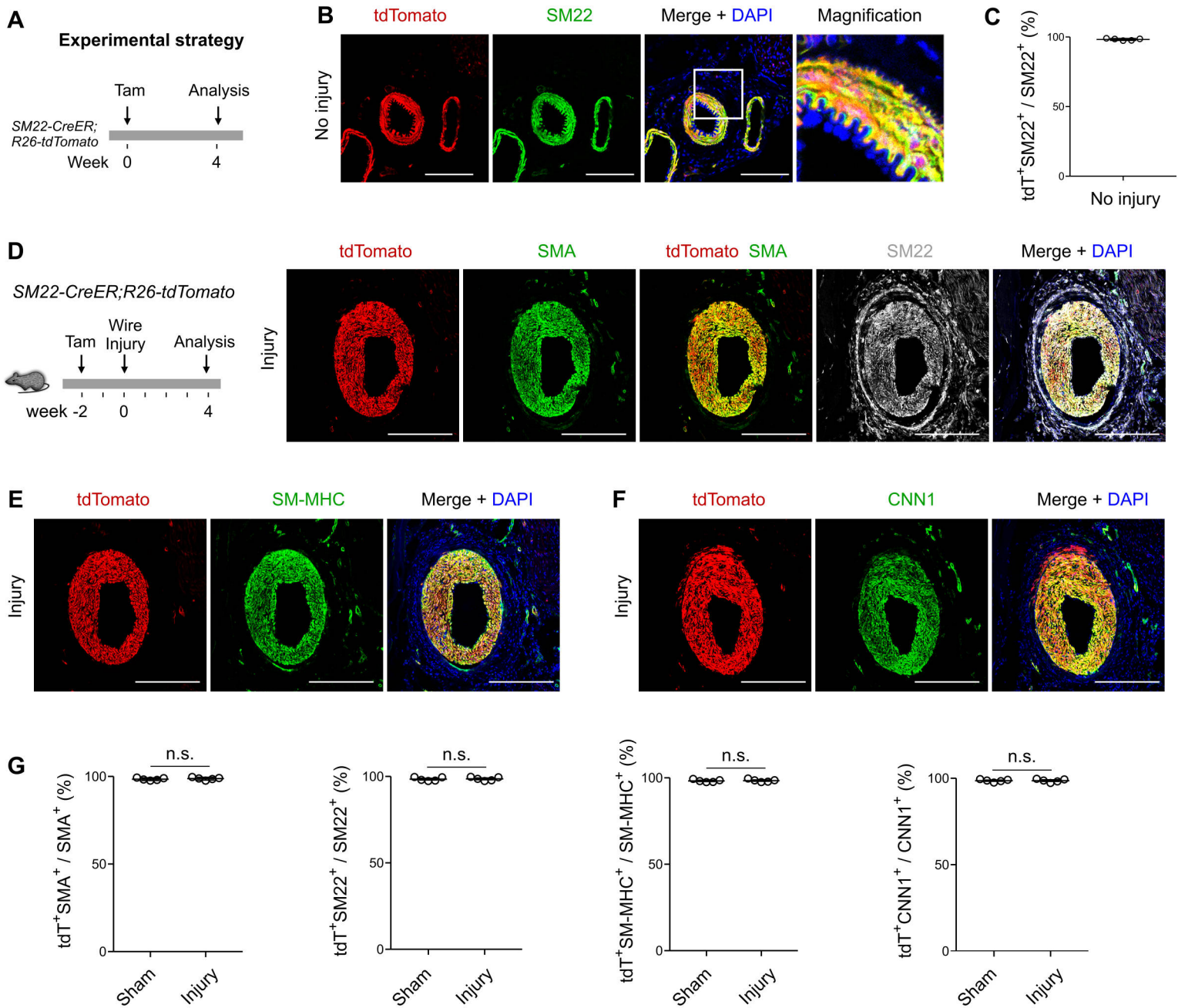


Figure S4 (Related to Figure 3). Lineage tracing of pre-existing smooth muscle cells in wire-induced injury model. (A) Schematic diagram showing genetic lineage tracing by *SM22-CreER;R26-tdTomato* after wire injury. **(B)** Immunostaining for *tdTomato* and smooth muscle cell markers *SM22* on non-injured artery. **(C)** Quantification of the percentage of *SM22*⁺ cells expressing *tdTomato*. Data are mean ± SEM; n = 5. **(D-F)** Immunostaining for *SMA*, *SM22*, *SM-MHC* or *CNN1* on femoral artery sections after wire-induced injury. **(G)** Quantification of the percentage of *SMA*⁺, *SM22*⁺, *SM-MHC*⁺ or *CNN1*⁺ SMCs that express *tdTomato* (*tdT*) in the artery wall. Data are mean ± SEM; n = 5; n.s., non-significant. Scale bars, white 100 μm. Each image is representative of 5 individual biological samples.

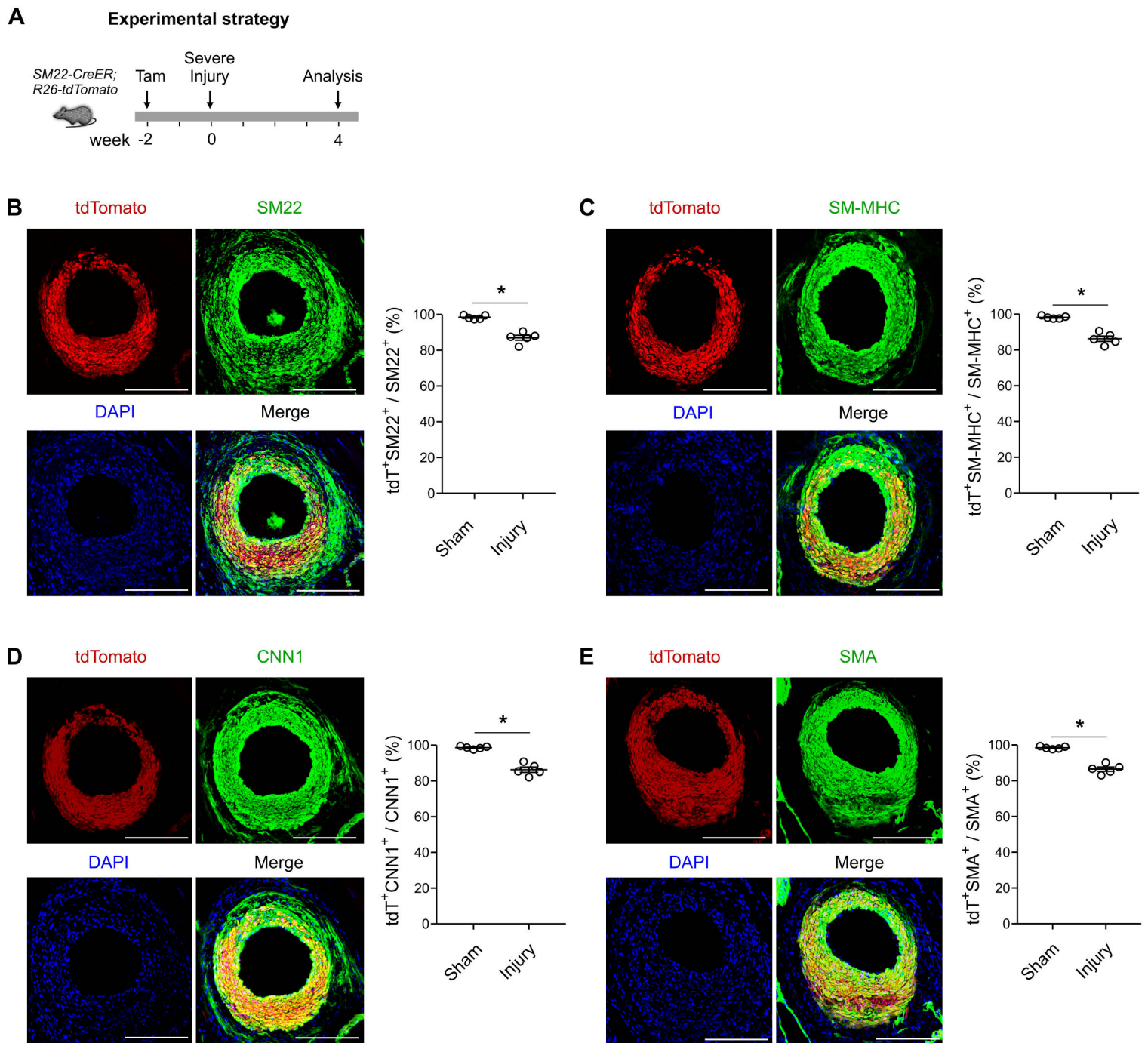


Figure S5 (Related to Figure 4). Smooth muscle contribution in arterial anastomosis model. (A) Schematic diagram showing genetic lineage tracing by *SM22-CreER;R26-tdTomato* in arterial anastomosis model. **(B-E)** Immunostaining for tdTomato and SM22, SM-MHC, CNN1 or SMA on tissue sections. Quantification of the percentage of smooth muscle cells expressing tdTomato (tdT). Data are mean \pm SEM; n = 5; **P* < 0.05. Scale bars, white 100 μ m. Each image is representative of 5 individual biological samples.

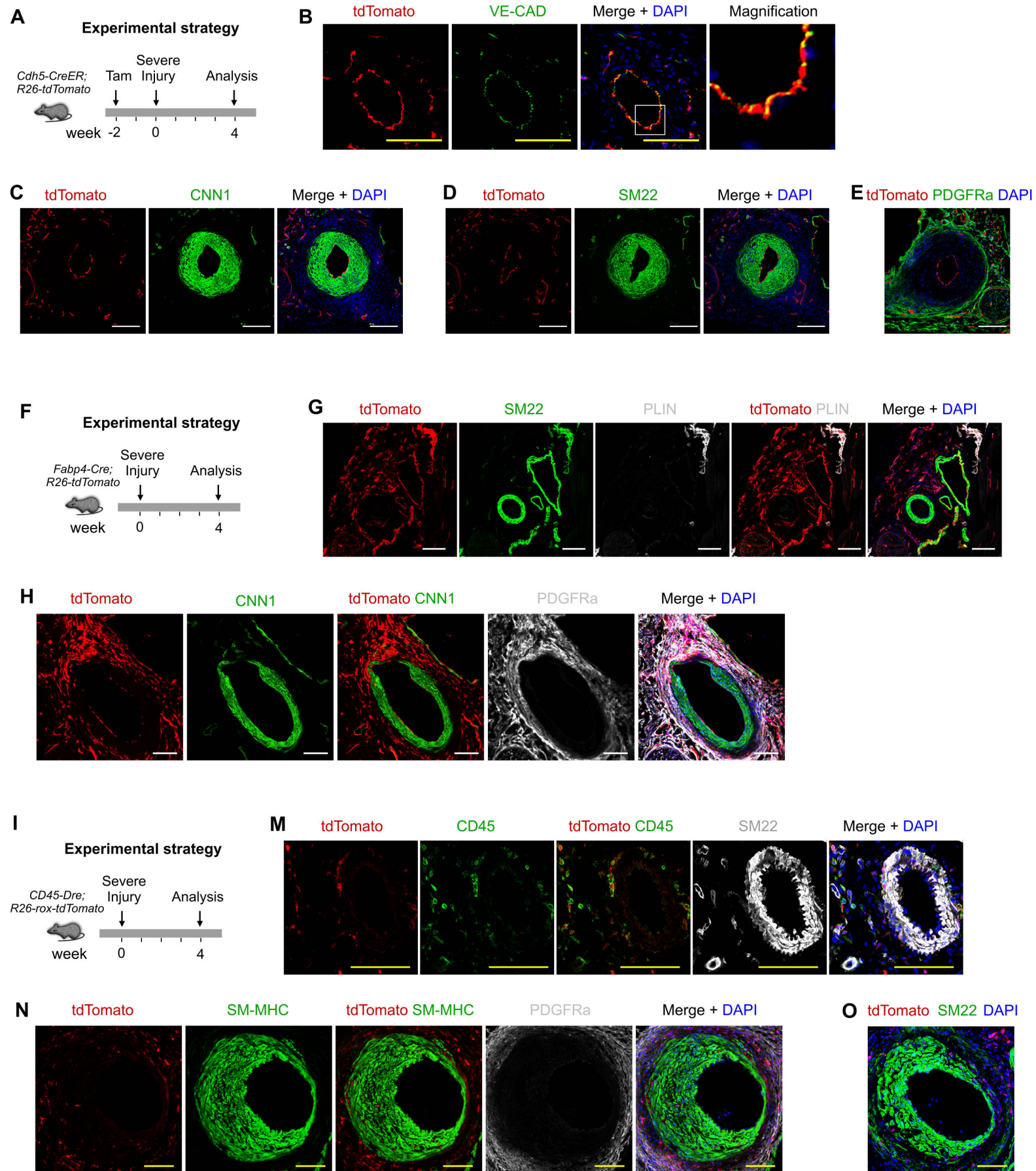


Figure S6 (Related to Figure 5). Endothelial cells fates in artery anastomosis model. (A,F,I) Schematic diagram showing genetic lineage tracing by *Cdh5-CreER;R26-tdTomato* (A), *FABP4-Cre;R26-tdTomato* (F), *CD45-Dre;R26-rox-tdTomato* (I) mouse. (B) Immunostaining for *tdTomato* and *VE-Cad* from femoral artery. (C,D) Immunostaining for *tdTomato*, *CNN1*, *SM22* on tissue sections. (E) Immunostaining for *tdTomato* and *PDGFRa* on tissue sections. (G) Immunostaining for *tdTomato*, *SM22* and adipocytes marker *Perilipin A* (*PLIN*) on femoral artery tissue. (H) Immunostaining for *tdTomato*, *CNN1*, and *PDGFRa* on tissue sections. (M) Immunostaining for *tdTomato*, *SM22* and *CD45* on femoral artery tissue. (N,O) Immunostaining for *tdTomato*, *SM-MHC*, *SM22* on tissue sections. N is the same section of Figure 5C. Scale bars, yellow 50 μ m, white 100 μ m. Each image is representative of 5 individual biological samples.

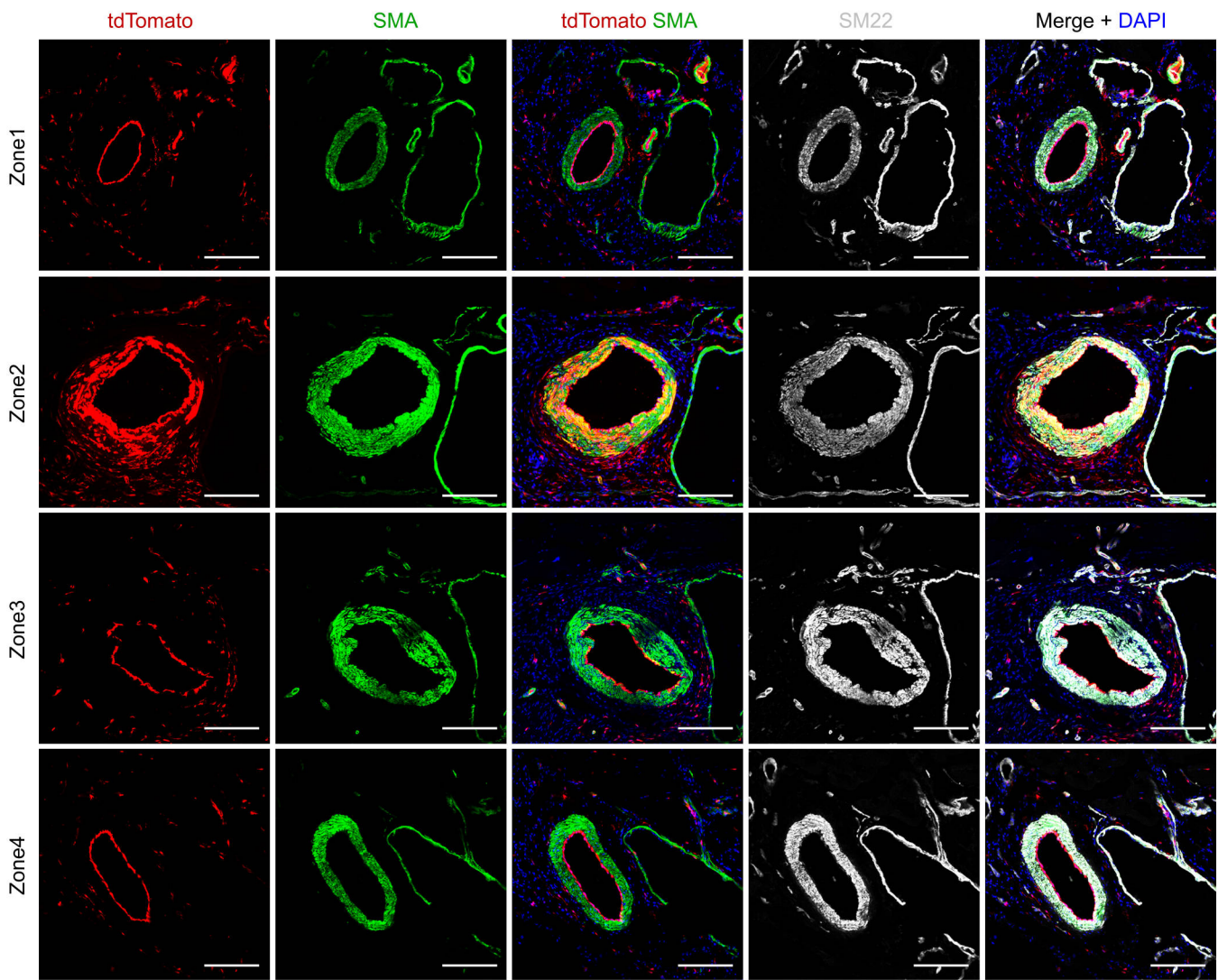


Figure S7 (Related to Figure 6). Sca1+ cells contribute significantly to smooth muscle at 12 weeks after injury. Immunostaining for tdTomato, SMA, SM22 on tissue sections of different segments of arteries after anastomosis model. Scale bars, white 100 μ m. Each image is representative of 5 individual biological samples.